Mechanisms of impurity effect and ductility enhancement of Mo and Cr alloys

N. Ma, and B.R. Cooper
Physics Department

C. Feng and B.S.-J. Kang
Mechanical and Aerospace Engineering Department
West Virginia University

UCR/HBCU Conference, Pittsburgh, June 5, 2007

DOE/NETL UCR Program, Contract No. DE-FG26-05NT42526

Background

Ductility improvement of Mo phase by inclusion of metal oxide dispersion (Schnibel 2003)

Experimental difficulties:

- Optimal dispersion **composition**
  - $MgAl_2O_4$, MgO, or other oxide candidates?
  - nano-size oxide? how to achieve uniform dispersion and prevent agglomeration?

Atomistic modeling can provide some answers to these questions to reduce experimental trial and error

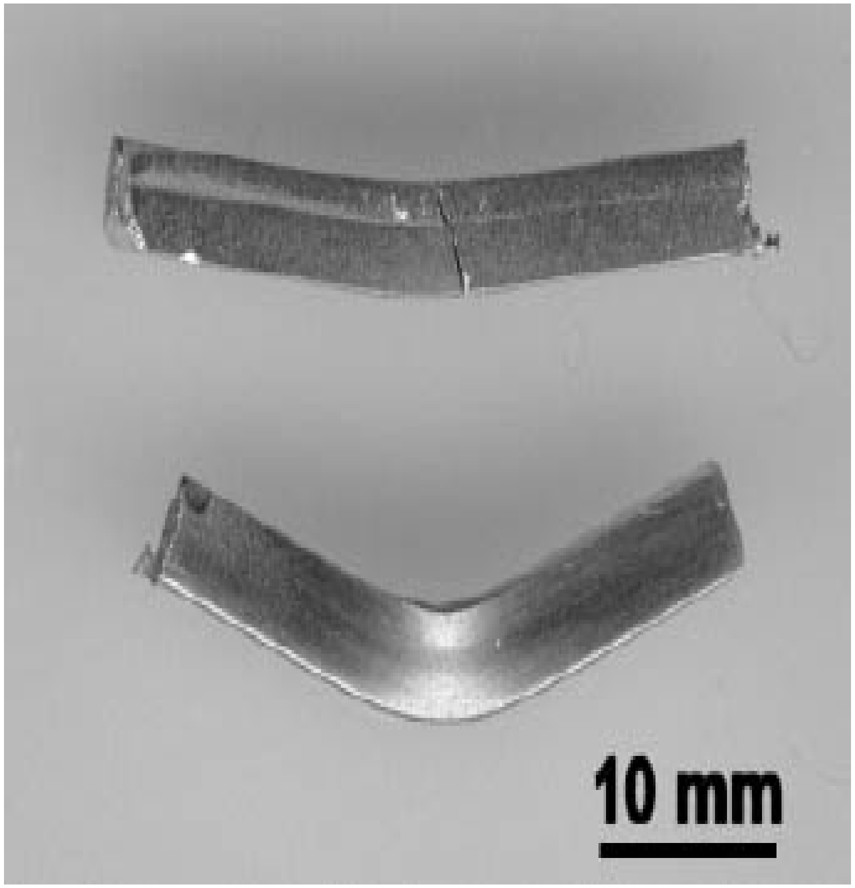

Mo with spinel dispersions: different procedures yield different results. (Schnibel, 2003)

Material Matrix

Materials received from Oak Ridge National Laboratory	
***Pure Cr, HP 2 hrs/1590C**	Cr-6TiO2, HP 2hrs/1590C
***Scruggs Cr-6MgO-0.5Ti (extrusion, 1300C) HP 2hrs/1590C**	Cr-6Y2O3, HP 2hrs/1590C
Cr-6MgO-0.5Ti, HP 2hrs/1590C	Cr-2MgO, HP 2hrs/1590C
Cr-6MgO-0.5Ti, sintered HP 2hrs/1590C	Cr-2ZrO2, HP 2hrs/1590C
Cr-6MgO-0.5Ti, HIP 1.5hrs/1590C	Cr-2TiO2, HP 2hrs/1590C
Cr-6MgO-1Ti, HP 2hrs/1590C	Cr-6La2O3, HP 2hrs/1590C
Cr-6MgO-2.2Ti, HP 2hrs/1590C	Cr-3MgAl2O4, HP 2hrs/1590C
Cr-6MgO-0.75Ti, HP 2hrs/1590C, extruded 1300C	Cr-Fe-MgO, 51.75Cr-42.44FE-5.66MgO-0.15La2O3wt%, extruded powders at 1300C
Cr-6MgO-0.75Ti, HP 3hrs/1590C, extruded 1300C	***Cast Re-(26-30)Cr wt% nominal**
Cr-6MgO, HP 2hrs/1300C	#695, MO, Mo powder (2~5um) HP/1hr/1800ºC/3ksi/Vacuum
Cr-6MgO, HP 2hrs/1450C	***#697, Mo-6wt%MgAl2O4, Mo powder (2-8um), MgAl2O4 (1-5um) HP/1hr/1800ºC/3ksi/Vacuum**
Cr-6MgO, HP 2hrs/1590C	#698, Mo-3wt%MgO, Mo powder (AEE, 2-8um) MgO, HP/1hr/1800ºC/3ksi/Vacuum
***Cr-6MgO(Nano), HP 2hrs/1500C**	***#678, Mo-3.4wt%MgAl2O4, Mo powder(2-8um) MgAl2O4(1~5µm),HP/1hr/1800ºC/3ksi/Vacuum**

Alloys received from M.P. Brady and J. H. Schneibel, ORNL; HP: Hot Pressing; *: alloys tested

Influence of impurity elements

Insufficient ductility mostly due to impurities (such as N, O, etc.)

- weaken the metal-metal bond
- precipitate or segregate as brittle oxides or nitrides

Ductility enhancement by MgO or $MgAl_2O_4$ spinel dispersions:

- Scruggs 1965: on Cr and Mo Alloys
  - Mechanism assumed to be impurity gettering by spinel phase
- Brady 2003 (detailed microstructural analysis): on Cr Alloys
  - No gettering effect found (impurities not detected in oxide phase)
    - $MgAl_2O_4$ is not as effective as MgO
    - Other metal oxides were tried with detrimental results
    - unclear whether MgO or $MgCr_2O_4$ is more effective
  - **Fundamental mechanism remains unknown**
    - Difficult to optimize the composition and size of dispersion material

The overall research objective is to understand and minimize the impurity effect for room-temperature ductility improvement of Mo- and Cr-based alloys by the inclusion of suitable nano-size metal oxide dispersions.

Task 1: Atomistic Modeling

To study mechanisms of impurity embrittlement of Cr- and Mo-based alloys and their room-temperature ductility enhancement by suitable metal oxides.

Task 2: In-situ Mechanical Property Measurement

To develop a micro-indentation measurement technique for quick assessment of material mechanical properties.

Task I: Atomistic Modeling

Mechanisms of impurity embrittlement of Cr- and Mo-based alloys and their room-temperature ductility enhancement by (nano-sized) metal oxides.

Objectives

- Probe ***microscopic*** mechanisms
  - Impurity embrittling due to N or O
  - Ductility enhancement effects of MgO or $MgAl_2O_4$

- Optimize performance
  - Optimal dispersion composition
  - Optimal size
  - Optimal processing condition, etc.

Approach overview

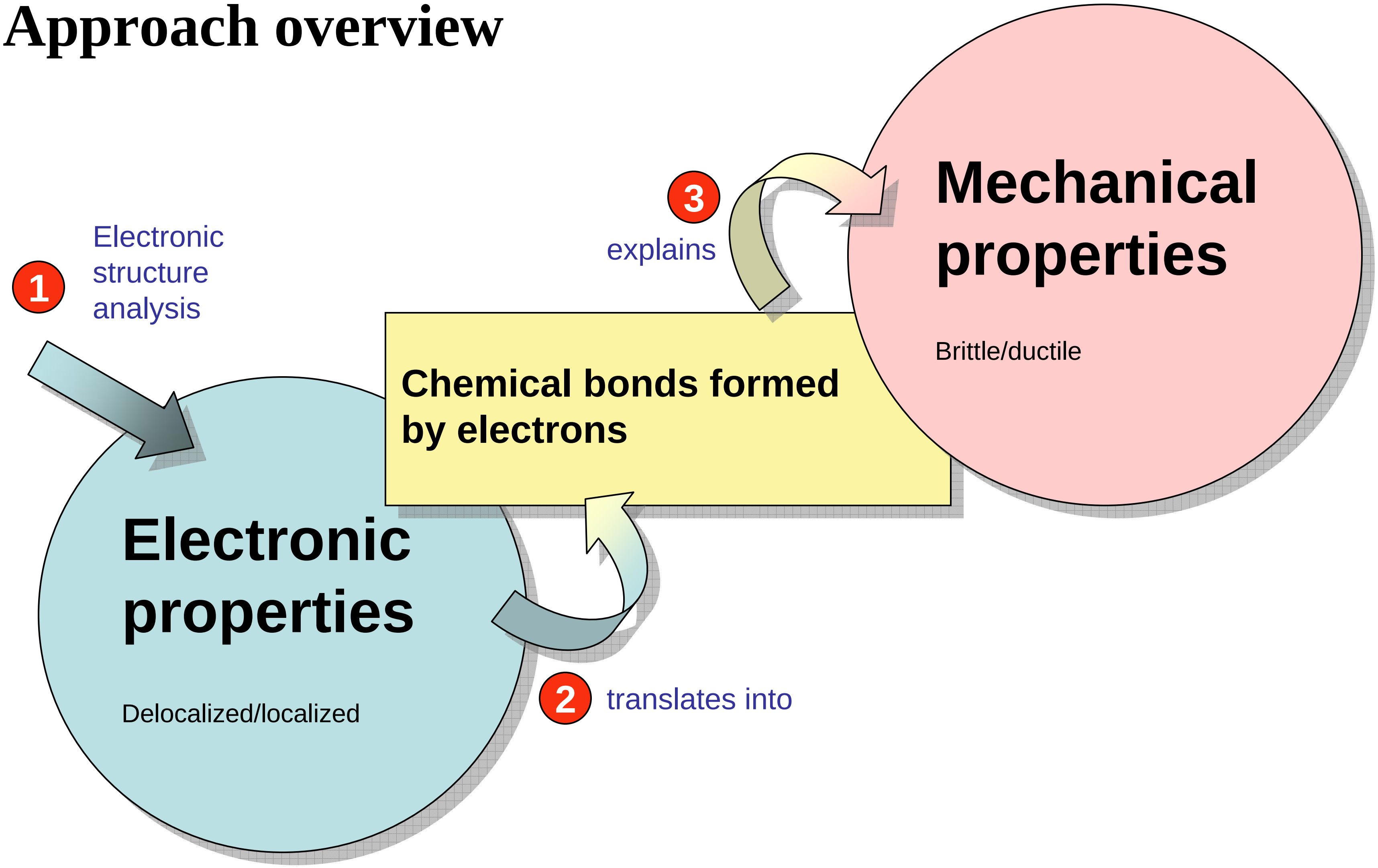

Outline

- **Theory:** Rice's criterion on ductility
- Results: Properties of electrons
- Results: Molecular dynamic simulations

Rice's criterion

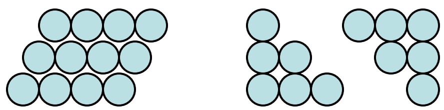

What matters are:

the characteristics of the chemical bonds

the properties of the valence electrons

How properties of electrons affect ductility

In brittle materials …

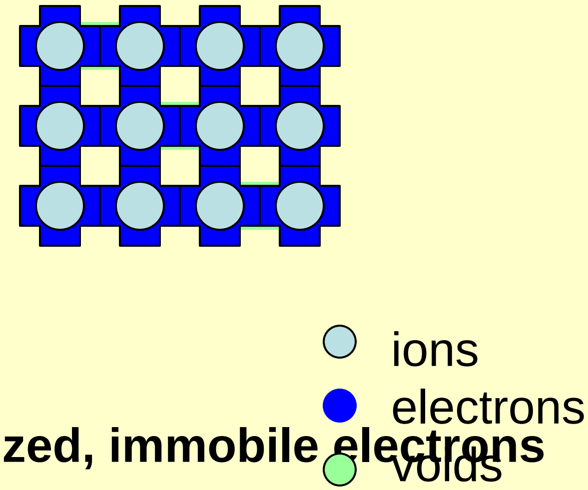

Localized, immobile electrons form rigid bonds → brittle

Localized around ions

Immobile (cannot fill the voids easily)

Delocalized, mobile electrons make flexible bonds → ductile

Theory: summary

Rice's criterion

Delocalized electrons	→	**ductile**
Mobile electrons	→	**ductile**
Flexible bonds	→	**ductile**

Outline

- Theory: Rice’s criterion on ductility
- **Results:** Properties of electrons
- Results: Molecular dynamic simulations

FP-LMTO
Ab-initio full-electron package

Price, Wills, and Cooper, Phys. Rev. B 46 (1992) 11368

Accurate

- Based on density functional theory
- Core electrons treated exactly
- Full potential in the interstitial area
- Most suitable for transition metals

Capable

- Electronic properties
- Force calculation / relaxation

Model systems

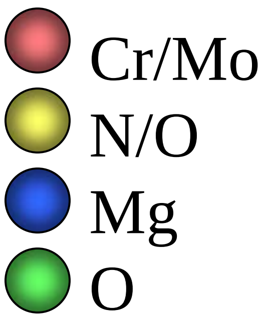

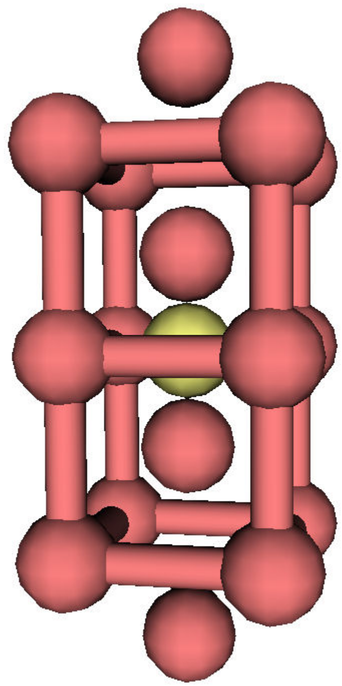

A. impurity embrittled system

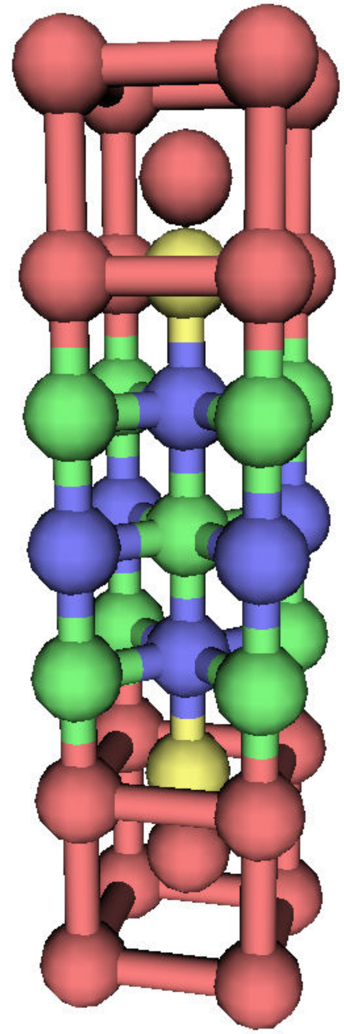

B. ductility enhanced system

Properties of electrons

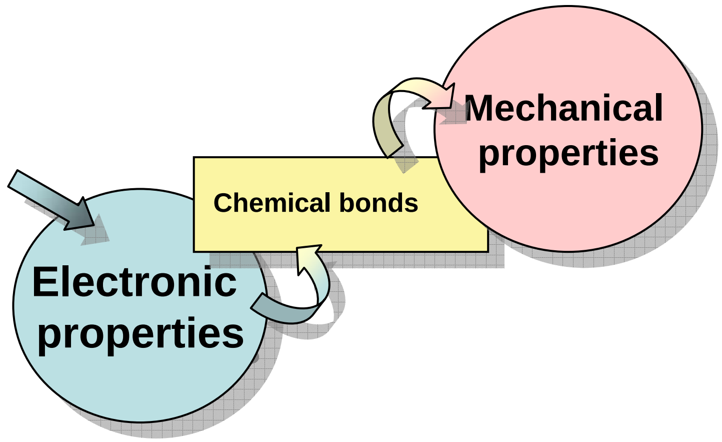

- **Space distribution**
  How localized/delocalized electrons are
- **Energy distribution**
  How easy electrons can be excited to mobile states
- **Angular momentum distribution**
  How rigid/flexible chemical bonds are

Charge density distribution

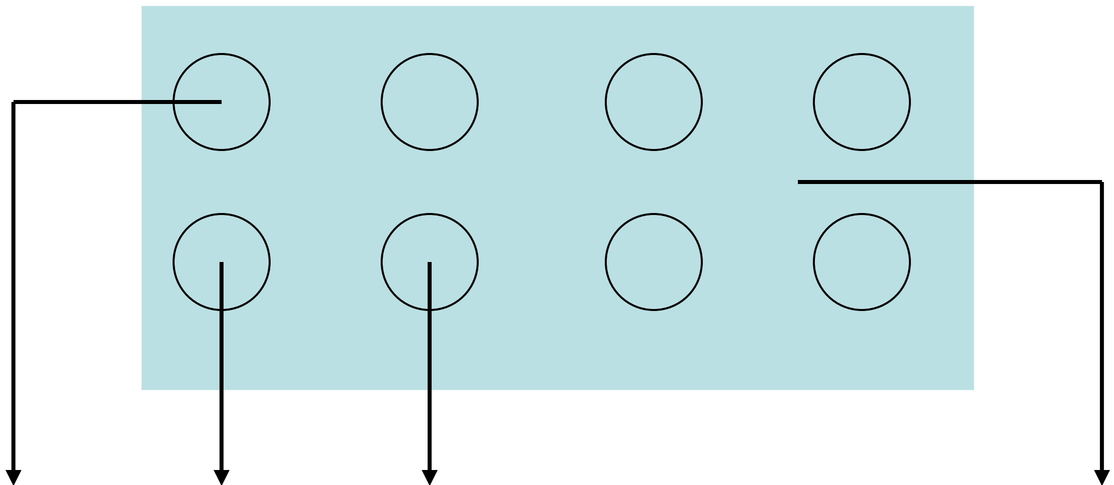

Muffin tin (MT) charge

- Localized within ions
  (yet still can be shared)
- Less mobile
- Partial contributor

Interstitial charge

- Fully delocalized
- Mobile ('itinerate')
- Main contributor to metallic bonds and ductility

Results: Interstitial charge (Cr alloys)

more interstitial charge → better ductility

Impurity imbrittled Cr

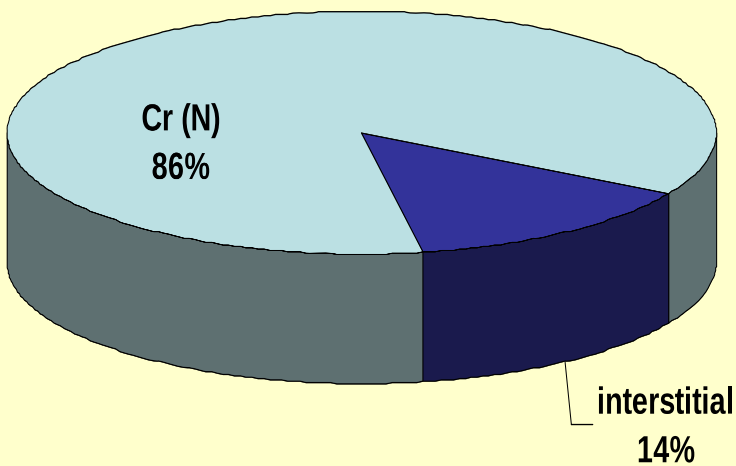

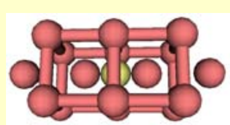

MgO ductilized Cr

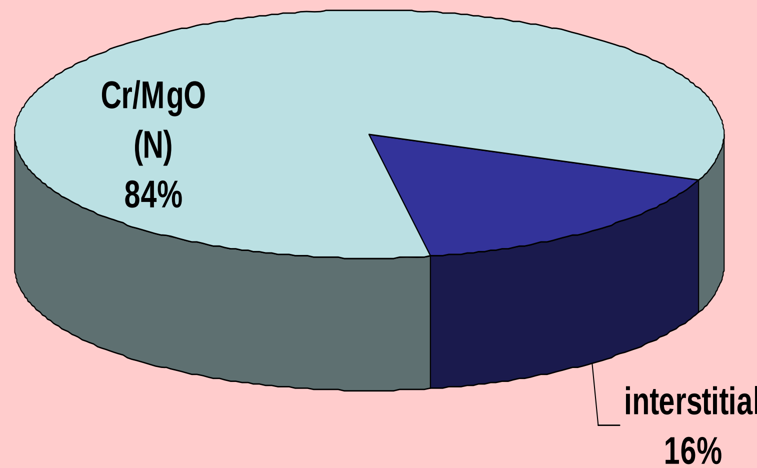

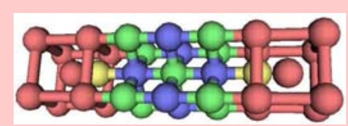

Results: Interstitial charge (Mo alloys)

more interstitial charge → better ductility

Impurity imbrittled Mo

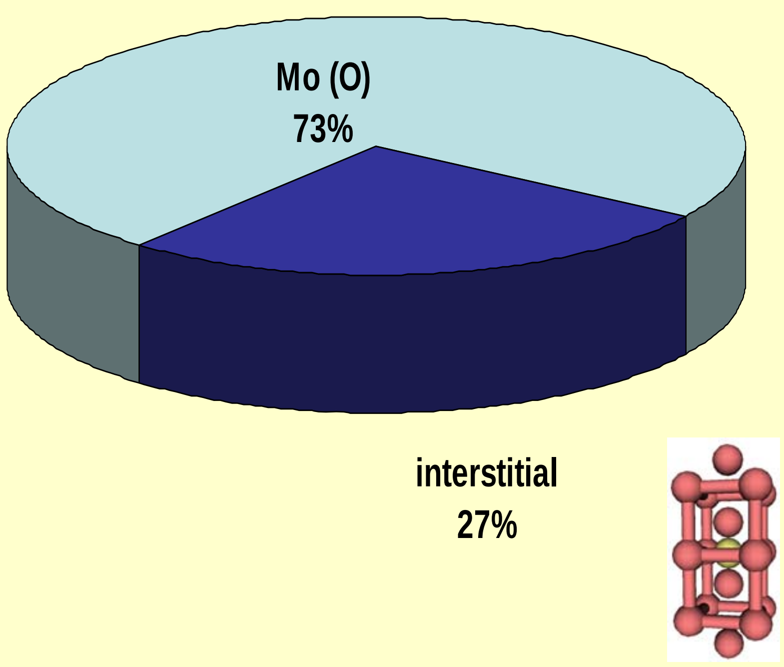

MgO ductilized Mo

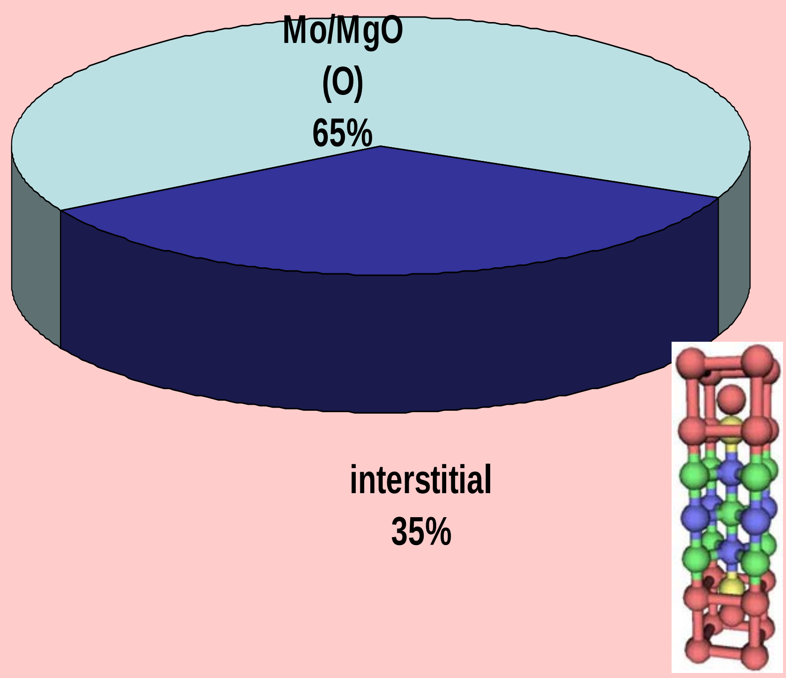

Results: Muffin-tin charge distribution

uniformly shared MT charge (less variance) → better ductility

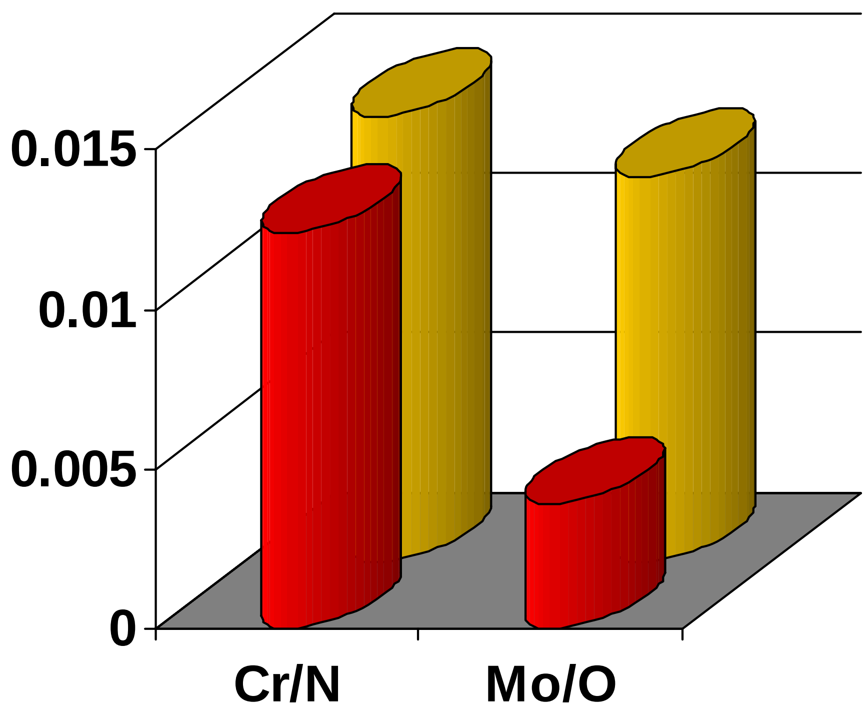

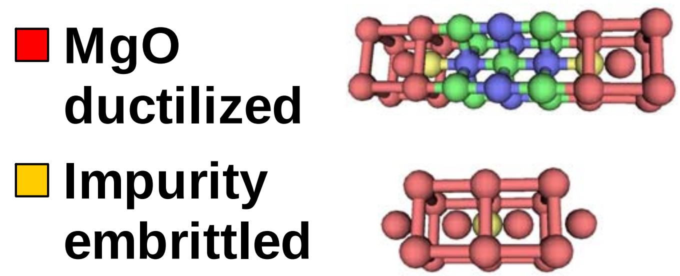

Variance of MT charge distribution among different Cr or Mo ions.

Properties of electrons

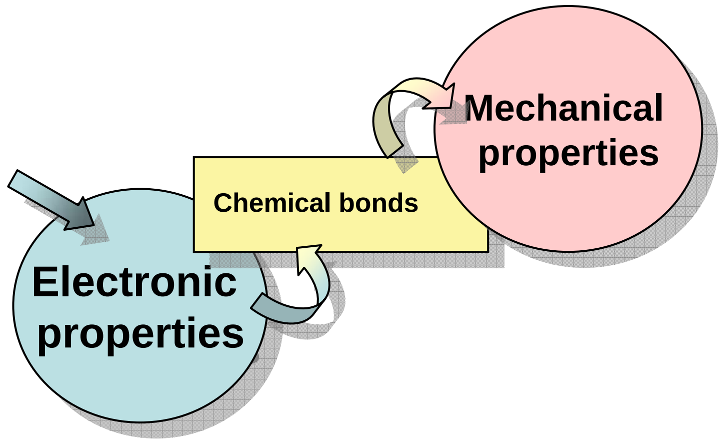

- **Space distribution**
  How localized/delocalized electrons are
- **Energy distribution**
  How easy electrons can be excited to mobile states
- **Angular momentum distribution**
  How rigid/flexible chemical bonds are

Density of states (DOS)

How easy electrons can cross the Fermi level to assume mobile states?

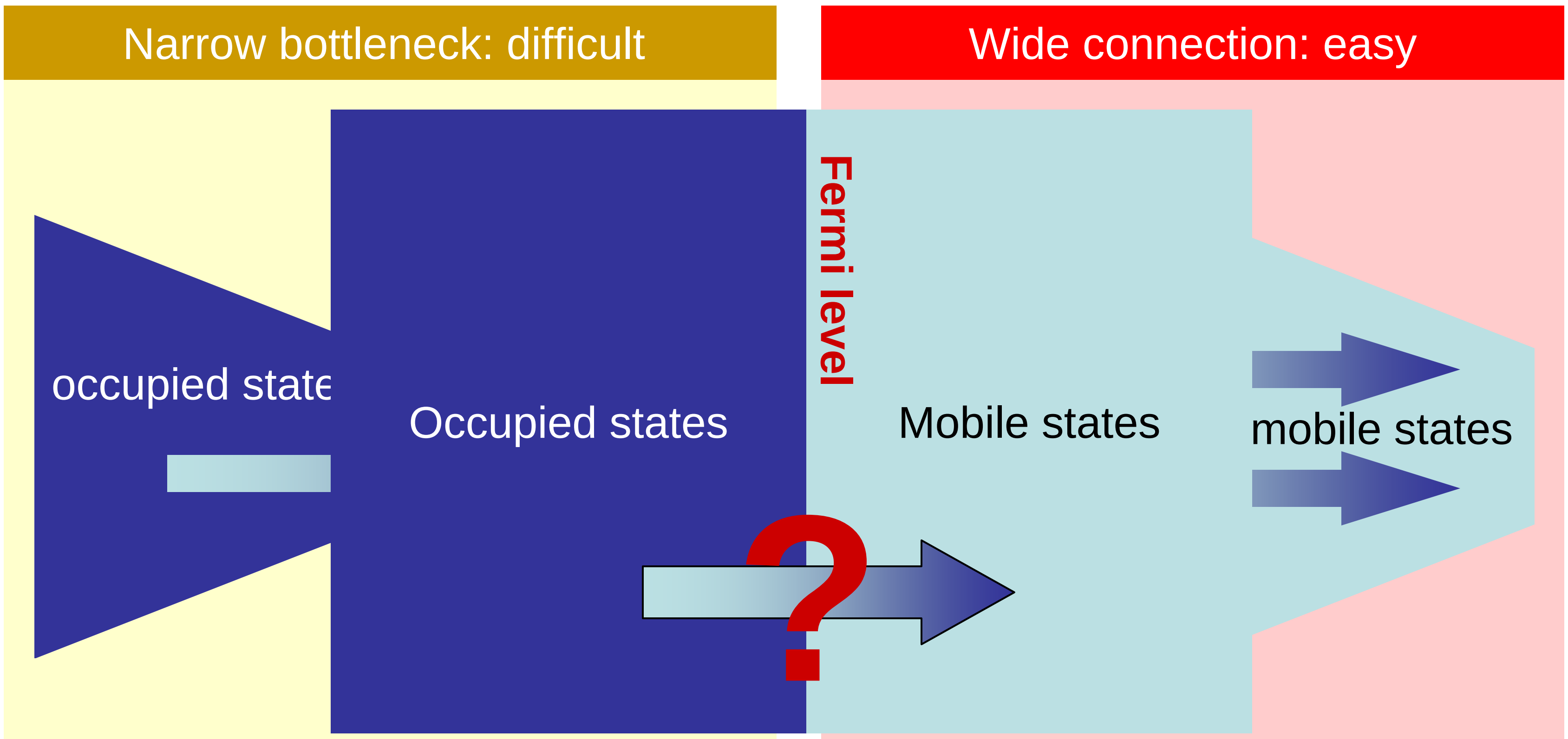

Results: DOS (Cr alloys)

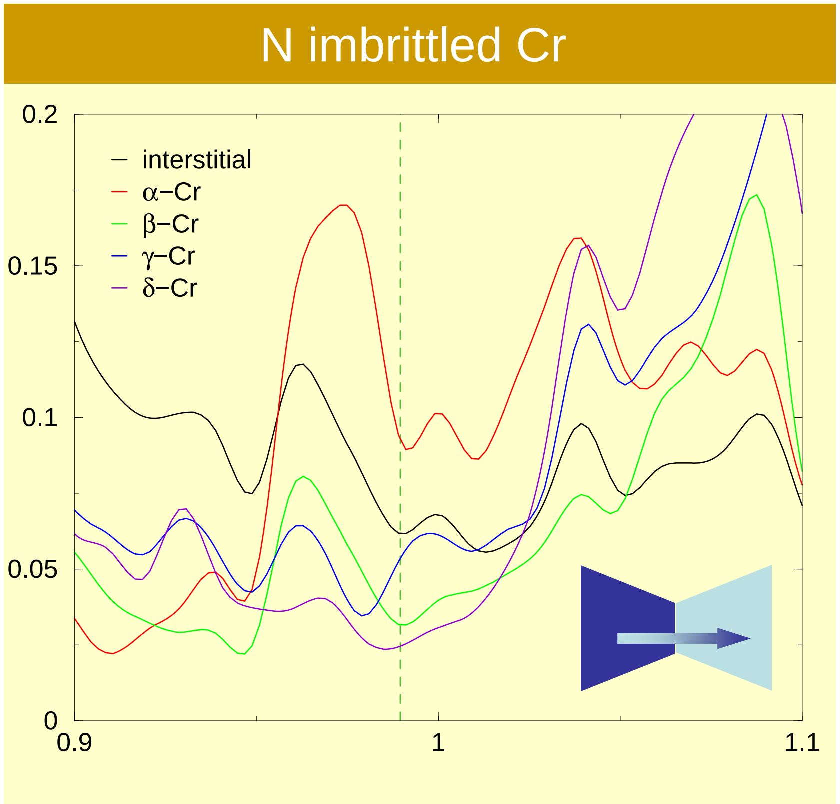

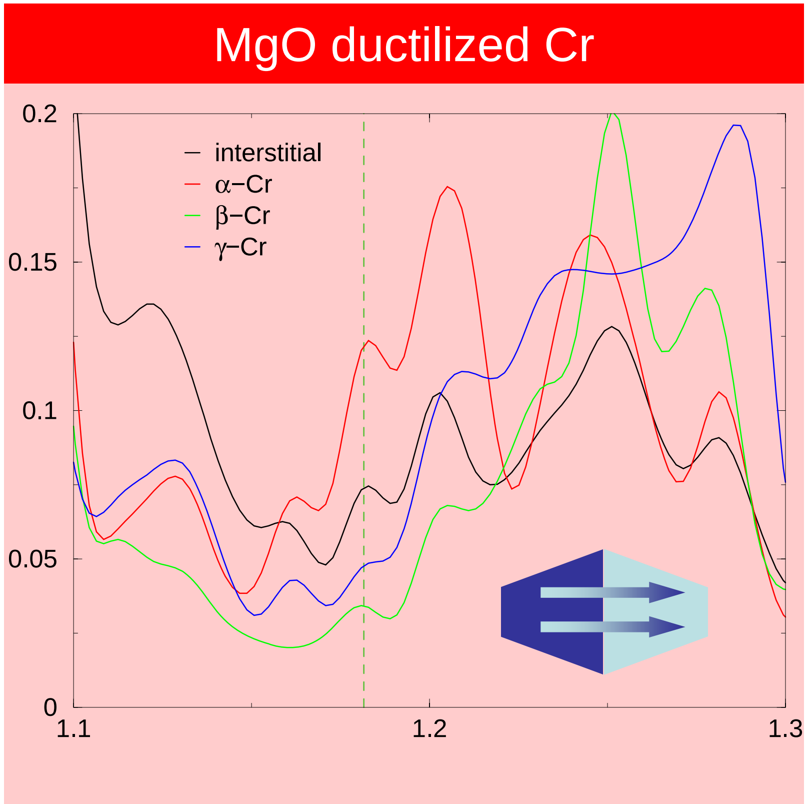

Results: DOS (Mo alloys)

O imbrittled Mo

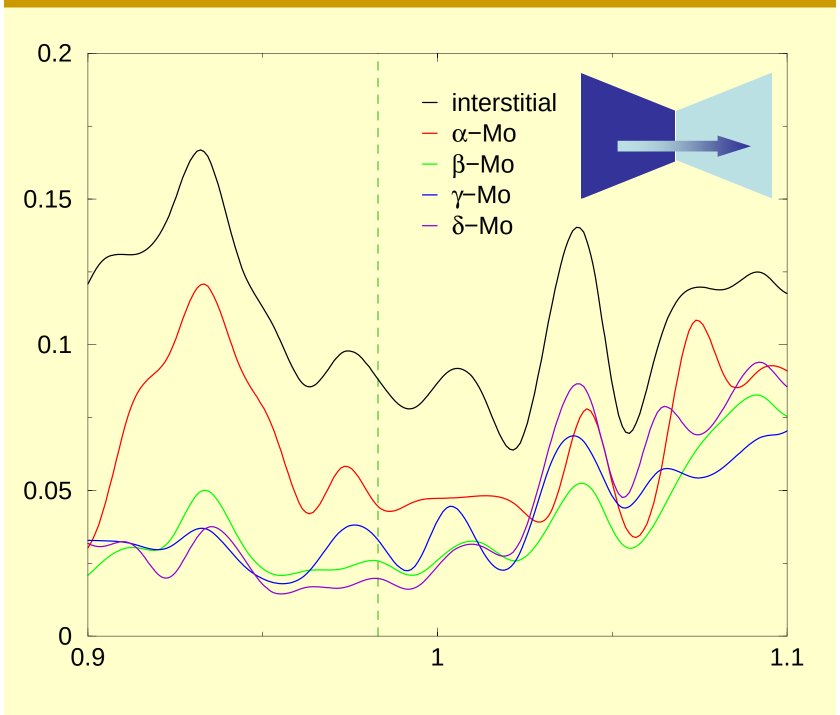

MgO ductilized Mo

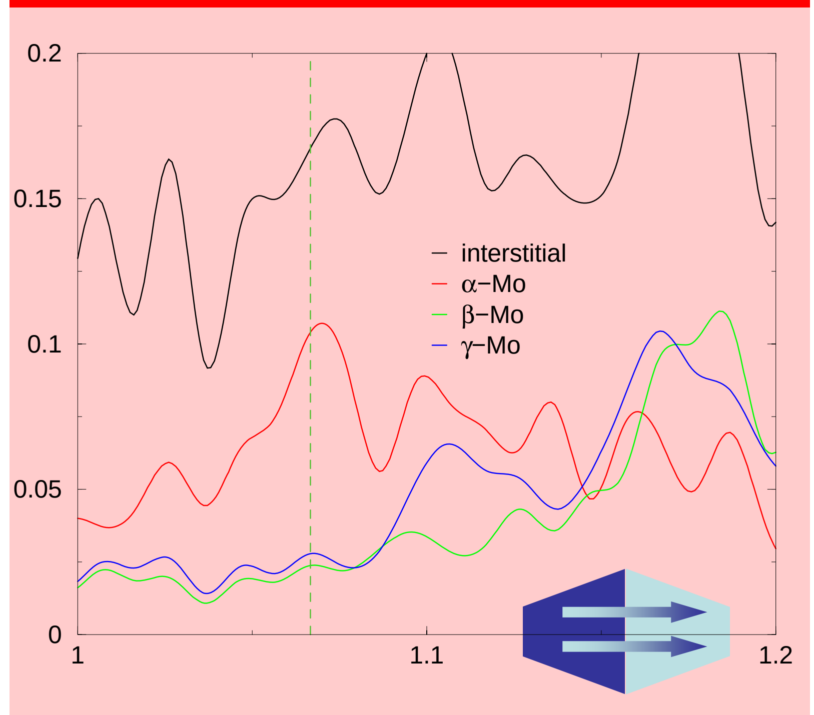

Properties of electrons

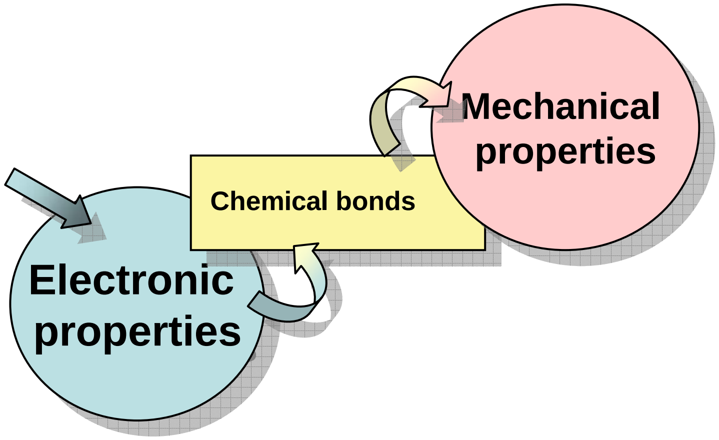

- **Space distribution**

  How localized/delocalized electrons are
- **Energy distribution**

  How easy electrons can be excited to mobile states
- **Angular momentum distribution**

  How rigid/flexible chemical bonds are

L-projection: s *(l=0)* vs. d *(l=2)*

d electron	s electron

Results: L-projected population

Charge (e)	N imbrittled Cr				MgO ductilized Cr		
	1st Cr	2nd Cr	3rd Cr	4th Cr	1st Cr	2nd Cr	3rd Cr
s-like	0.172	0.260	0.204	0.206	0.256	0.297	0.245
d-like	3.772	3.970	3.603	3.585	4.137	3.998	3.734
s/d %	4.6	6.5	5.7	5.7	6.2	7.5	6.6

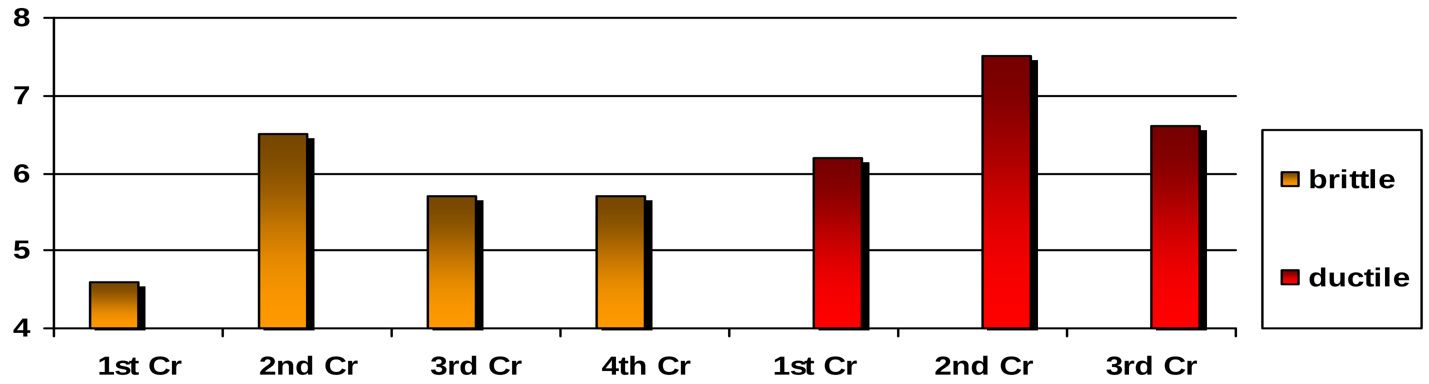

Less s-electrons More s-electrons

Results: L-projected energy

Energy Ryd.)	O embrittled Mo				MgO ductilized Mo		
	1st Cr	2nd Cr	3rd Cr	4th Cr	1st Cr	2nd Cr	3rd Cr
E* 4s	1.004	0.954	1.078	1.077	0.837	0.940	1.058
E* 3d	0.808	0.730	0.854	0.849	0.868	0.934	1.047
ΔE	0.20	0.22	0.22	0.23	-0.03	0.01	0.01

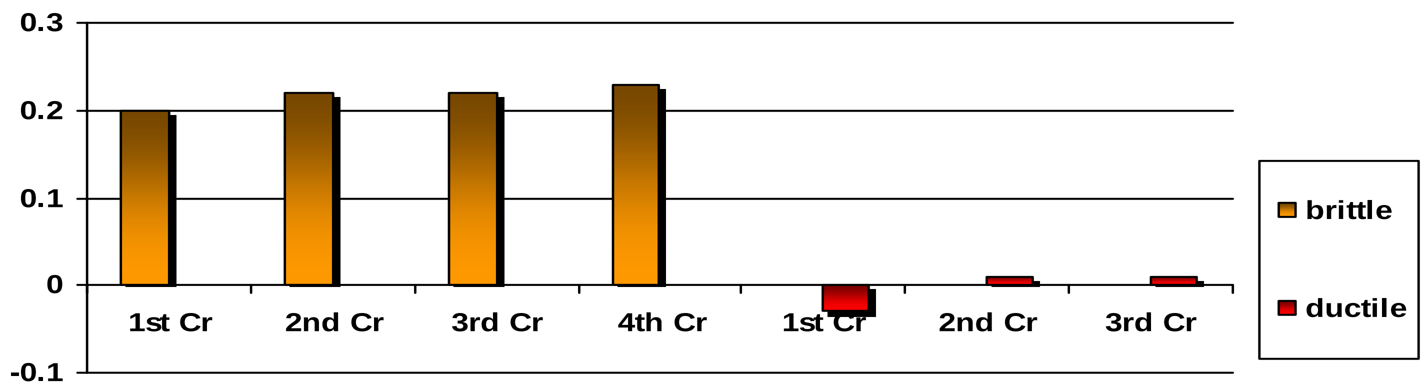

Higher s level **Lower s level**

Results: Band structure

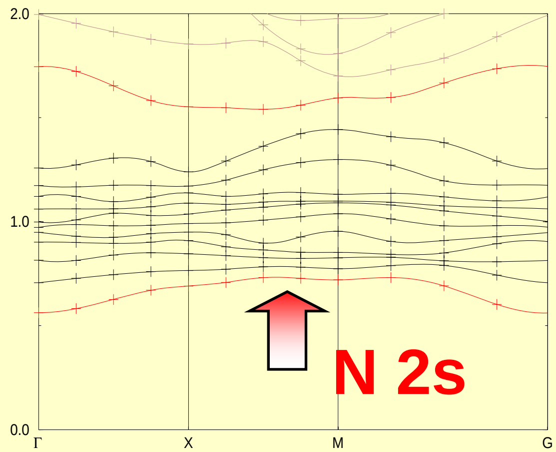

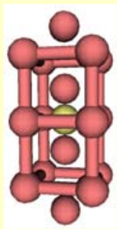

s band is pushed up by N's 2s band (not shown) from below, therefore becomes less populated → reduced s-partition and brittle system

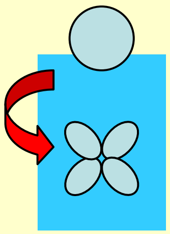

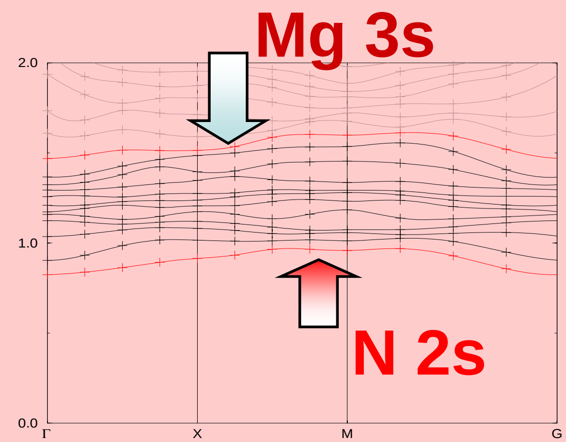

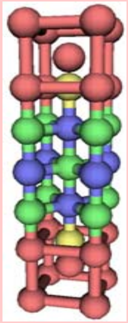

N's up-pushing effects are balanced by Mg's 3s bands from above, bringing Cr's s band back to the "normal" position → restored s-partition and ductile system

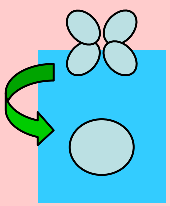

Summary: Properties of electrons

What has been achieved?

Identified ***microscopic*** criteria
to predict **brittle/ductile** properties

These criteria can

*Explain the **mechanism***
*Be used in larger scale simulations to **optimize** performance*

Outline

- Theory: Rice’s criterion on ductility
- Results: Properties of electrons
- **Results:** Molecular dynamic simulations

FIREBALL
Ab-initio tight-binding package

Lewis, Glaesemann, Voth, Fritsch, Demkov, Ortega, Sankey, Phys. Rev. B 64 (2001) 195103

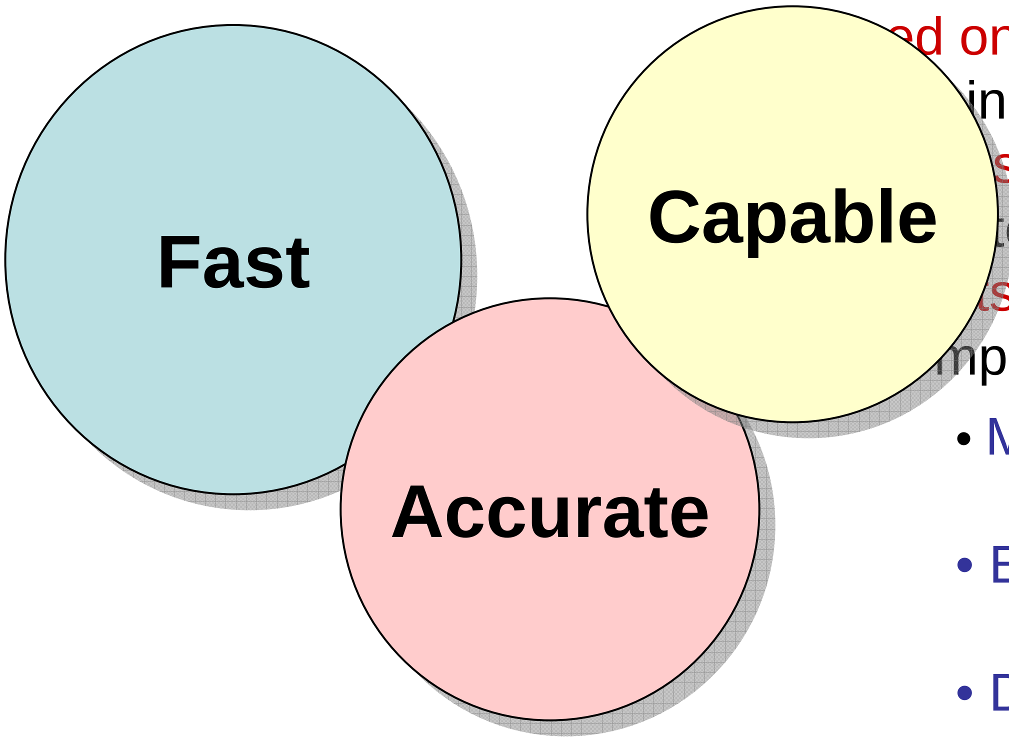

ed on density functional theory
inimal basis set
sistent charge density
tegrals are pre-computered
s for charge transfer effects
mputing, order-N algorithms

- Much larger (nano) system
- Electronic properties
- Dynamic simulation

Result: Molecular dynamics (Cr/MgO with N)

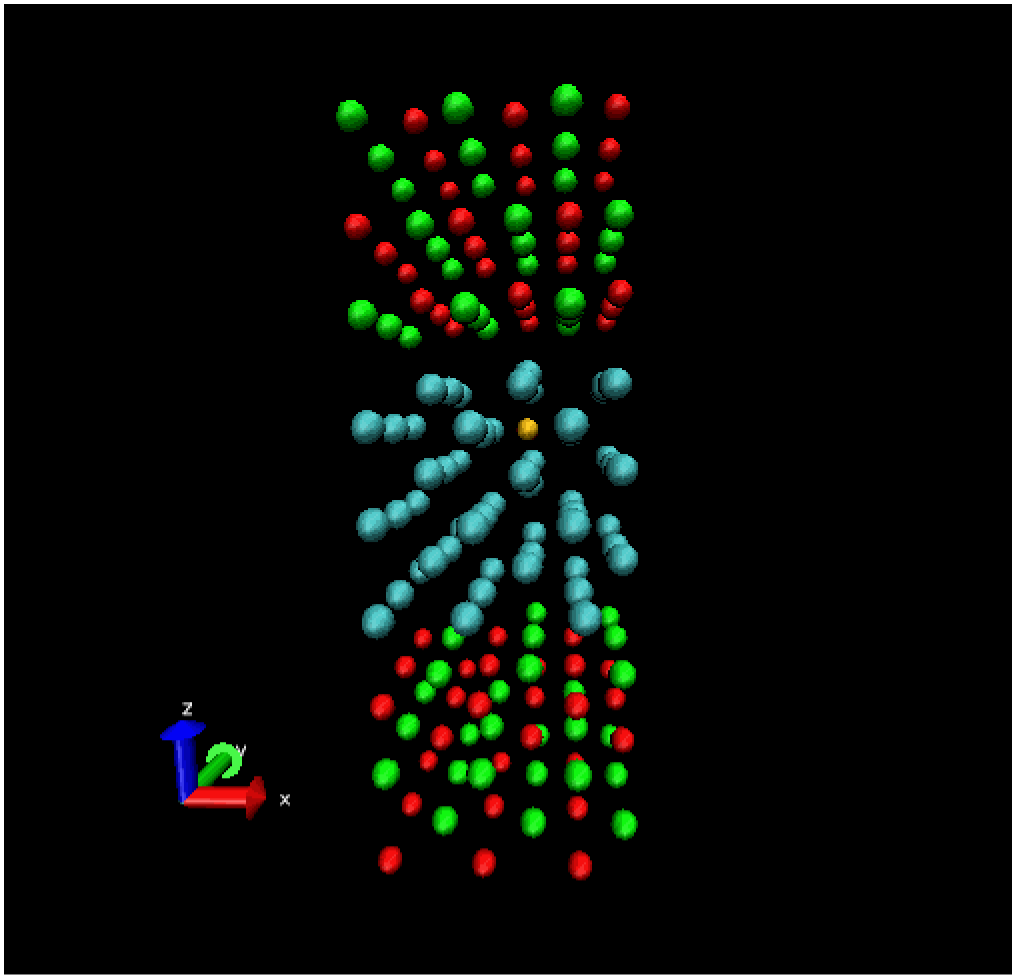

- Cr
- N
- Mg
- O

163 atoms

Constant Temperature (600 K)

Diffusion time ~1ps (10^{-12}s)
Diffusion length ~ 2A

Result consistent with Brady's experiment

Analysis: Charge density distribution and DOS (Cr/MgO with N, initial and final configurations)

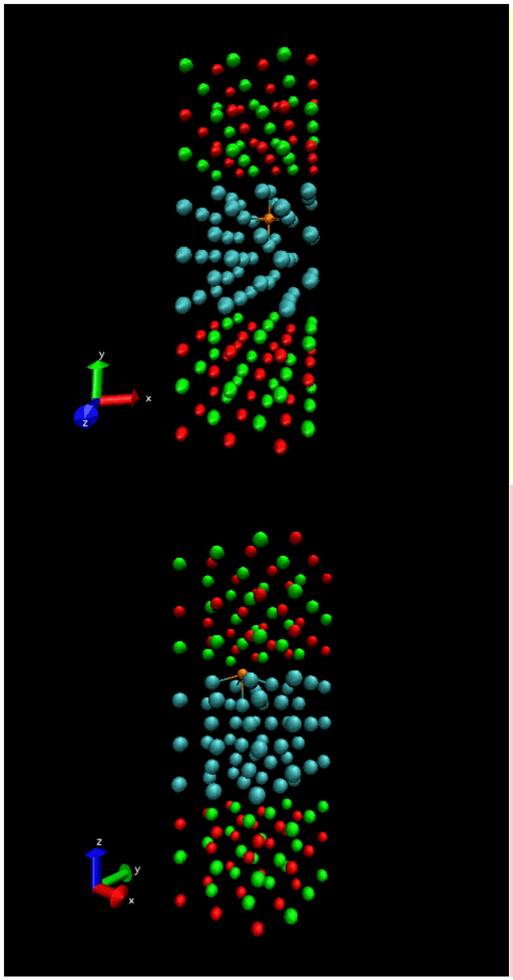

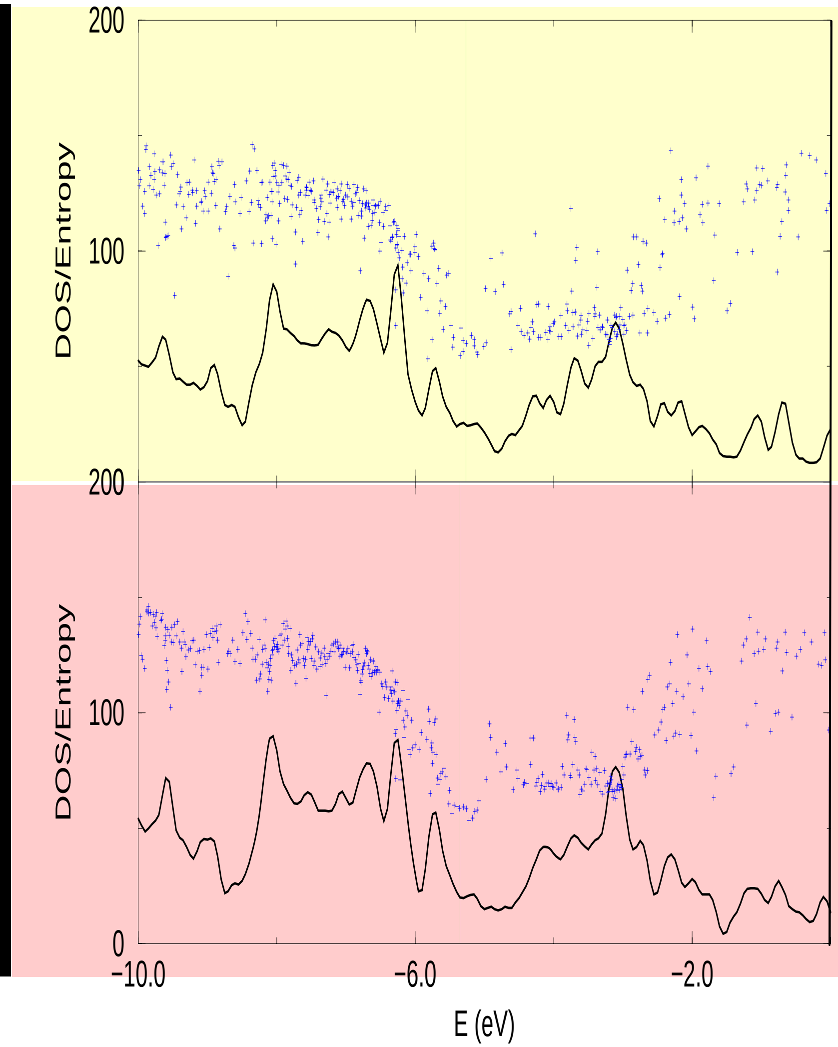

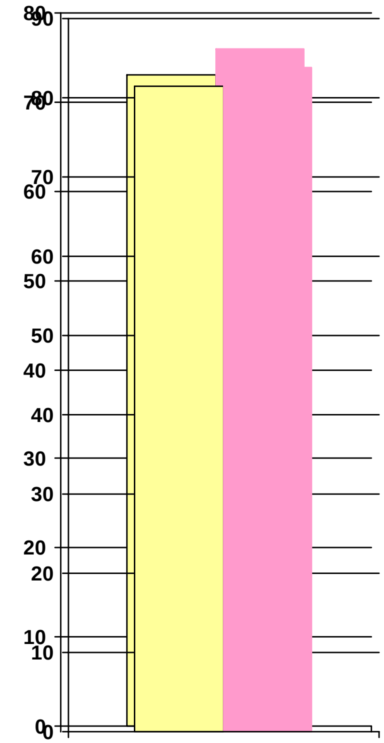

Avg. entropy within +/- 1eV of Fermi level

Result: Molecular dynamics ($Cr/MgAl_2O_4$ with N)

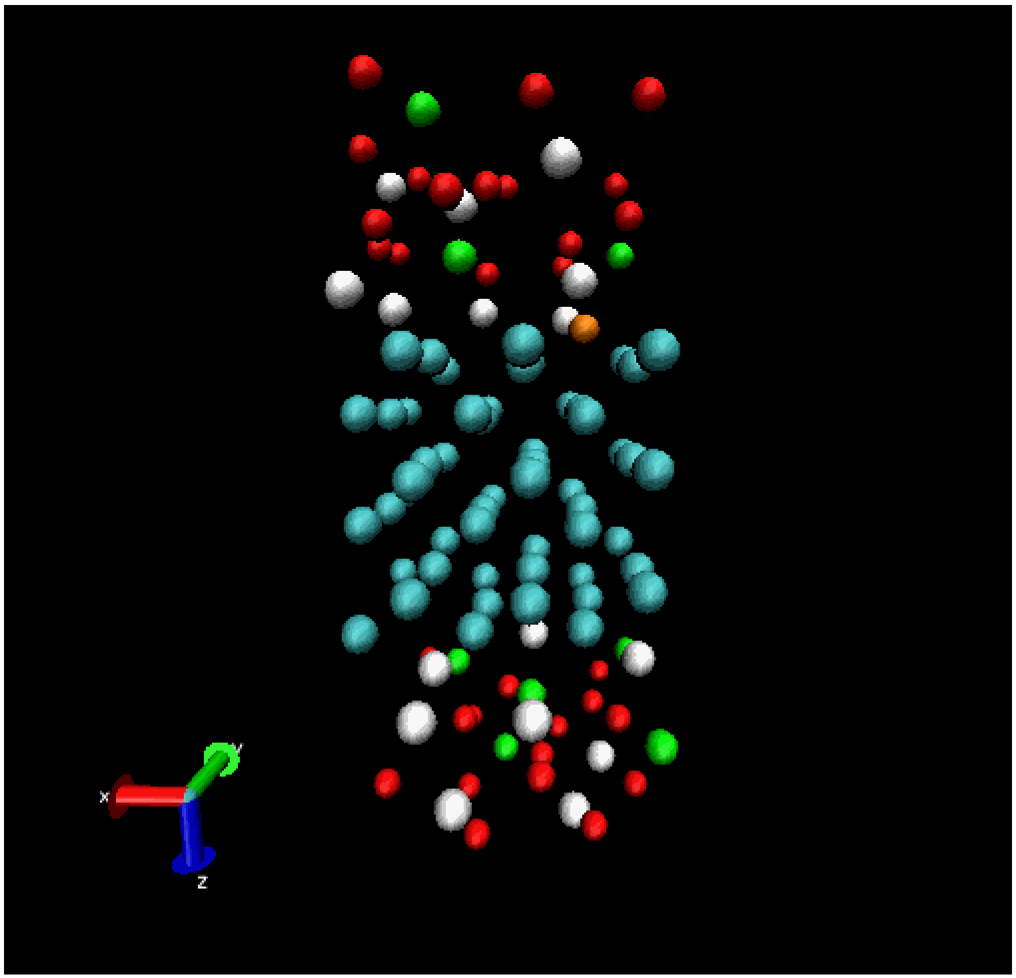

Cr
N
Mg
Al
O

111 atoms

Constant Temperature
(600 K)

Diffusion time ~1ps (10^{-12}s)
Diffusion length ~ 2A

Result: Molecular dynamics ($Mo/MgAl_2O_4$ with O)

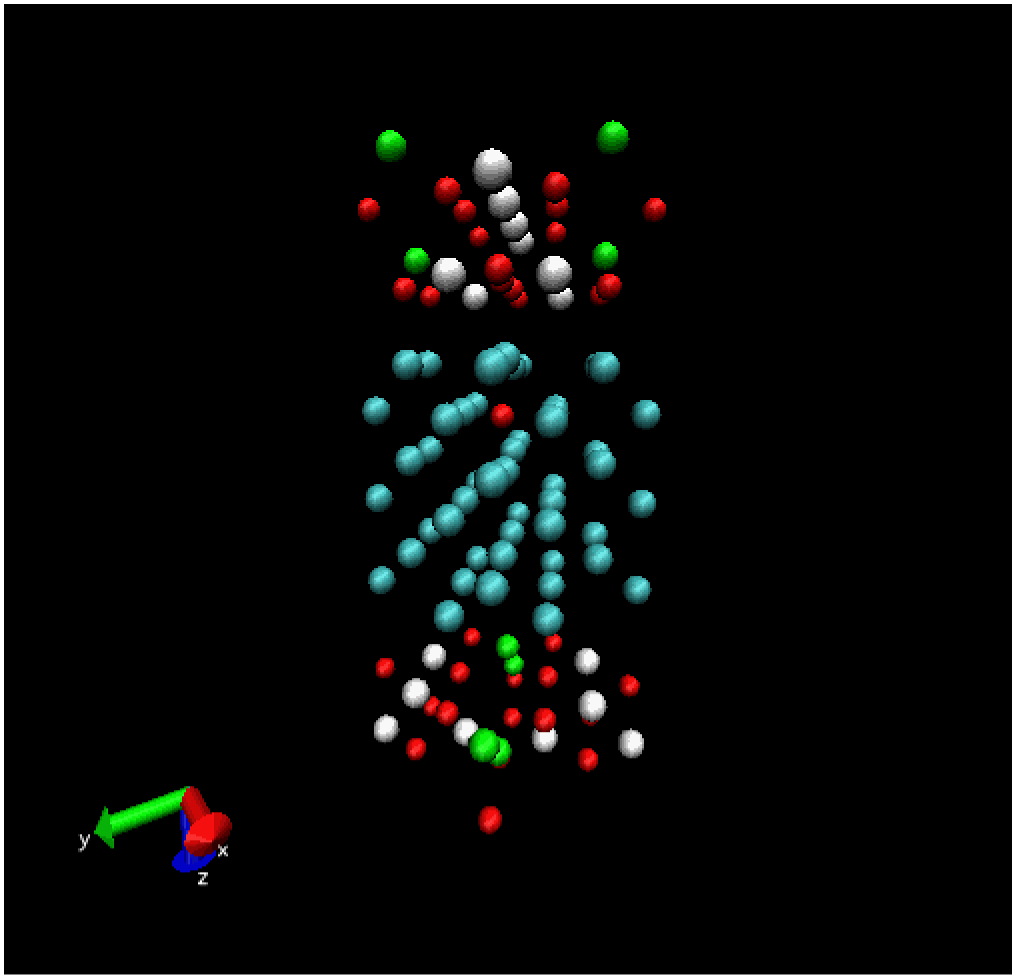

- Mo
- Mg
- Al
- O

105 atoms

Constant Temperature (600 K)

Simulation time ~1.6ps

No significant oxygen diffusion is observed. Results support Schneibel's conclusion.

Summary: Molecular dynamics simulation

Cr-based systems: *Observed possible impurity gettering*

- N diffused from inside the matrix to the interfacial boundary
- Charge distribution and DOS properties indicate improved ductility
- Results in consistency with Brady's experimental work:

  "impurity management effects"

  *Brady, et.al. Mat. Sci. & Eng. A, **358**, 243 (2003)*

Mo-based systems: *No impurity gettering observed*

- O impurity stable in matrix after 1.6 ps (1600 steps)
- Significant relaxation in the spinel phase due to lattice mismatch
- Results support Schneibel's conclusion

  "grain size optimization effects"

  *Schneibel, et.al. Metall. & Mater. Trans. **34A**, 25 (2003)*

Conclusions

Identified ***microscopic*** criteria
to predict **brittle/ductile** properties

These criteria can

*Explain the **mechanisms***

*Be used in larger scale simulations to **optimize** performance*

Observed possible tendency for **impurity gettering**

This work demonstrates the capability of

*Studying the **dynamic effects***

Carrying out large scale simulations

Third-Year Research

Larger system size (nano scale simulation)

- Dispersion particle size effects
- Dynamic effects (quenching, diffusion, etc.)

Other metal oxide composition

- $MgAl_2O_4$ or other to achieve better ductility?

Same technique used here can be applied in **other areas**

- S/P/As effects on Ni annode material in SOFC

Task 2: In-situ mechanical property measurement

Outline

- Micro-indentation Technique Development
  - Gen I: Transparent Indenter Measurement (TIM) Technique
  - Gen II: Simplified TIM Technique
  - **Gen III**: Multi-partial unloading indentation technique
  - **Capability:** Young's modulus, hardness, stress-strain curve ofalloys or thin-film coating, surface stiffness response measurement of multi- layers structures

- Ductile/Brittle assessment using indentation technique
  - Indentation-induced surface cracking
  - Surface profile/slip lines/shear bands

Materials Matrix

(Alloys received from M.P. Brady and J. H. Schneibel, ORNL)

#678, Mo-3.4wt%$MgAl_2O_4$: 1800°C/4hr/3ksi/Vacuum, Mo powder 2-8μm, $MgAl_2O_4$, 1-5μm

#696, Mo-3.0wt%$MgAl_2O_4$: 1800°C/1hr/3ksi/Vacuum, Mo powder 2-8μm, $MgAl_2O_4$, 1-5μm

#695, Mo only : 1800°C/1hr/3ksi/Vacuum, Mo powder 2-8μm

#697, Mo-6.0wt%$MgAl_2O_4$: 1800°C/1hr/3ksi/Vacuum, Mo powder 2-8μm, $MgAl_2O_4$, 1-5μm

#698, Mo-3wt%MgO : 1800°C/1hr/3ksi/Vacuum, Mo powder 2-8μm, MgO, 1-5μm

Cast Re-(26-30) Cr wt% nominal

(Powder mix prepared at WVU and sent to J.H. Schneibel for vacuum hot-pressed)

Mo-5.0wt%$MgAl_2O_4$: 1800°C/0.5hr/3ksi/Vacuum

Mo-5wt%MgO : 1800ºC/1.0hr/3ksi/Vacuum

Mo-5.0wt%TiO_2 : 1700°C/0.5hr/3ksi/Vacuum

(WVU $MgO_{0.05}Mo_{0.95}$, $TiO_{2\ 0.05}$ $Mo_{0.95}$, $MgAl_2O_{4\ 0.05}$ $Mo_{0.95}$ Powder Mixes)

(1) 95 g of Mo powder (65 nm nominal) was mixed in ethyl alcohol and sonicated for 10 minutes using a high intensity sonicator (VC 600) in the presence of Argon.

(2) Then 5 g of MgO or TiO_2 or $MgAl_2O_4$ powder (20 nm nominal) was added slowly to the Mo solution with continuous sonication. The total mixture was sonicated for 1 hour in Argon atmosphere.

(3) The solution was kept at room temperature in Argon-filled glove box to let the ethanol evaporate for 24 hours. The remaining alcohol was removed by drying the product in vacuum.

(4) The dried powder was kept in Argon filled glove box and packed in a bottle in the presence of Argon.

Gen I: Transparent Indenter Measurement (TIM) Technique

Optical Principle

- –Transparent indenter design
    - –Direct contact radius measurement
    - –Direct out-of-plane deformation measurement
- –Integrated phase-shifting technique

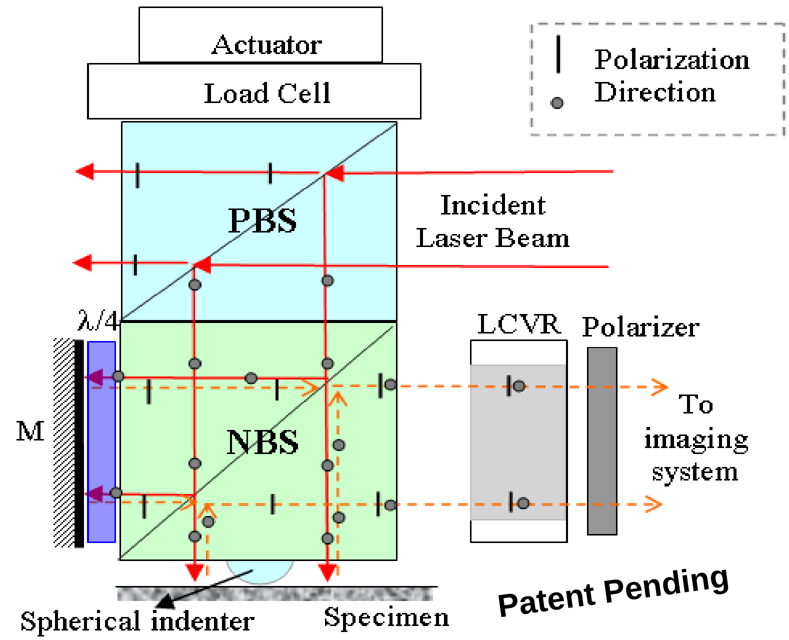

Laboratory Setup

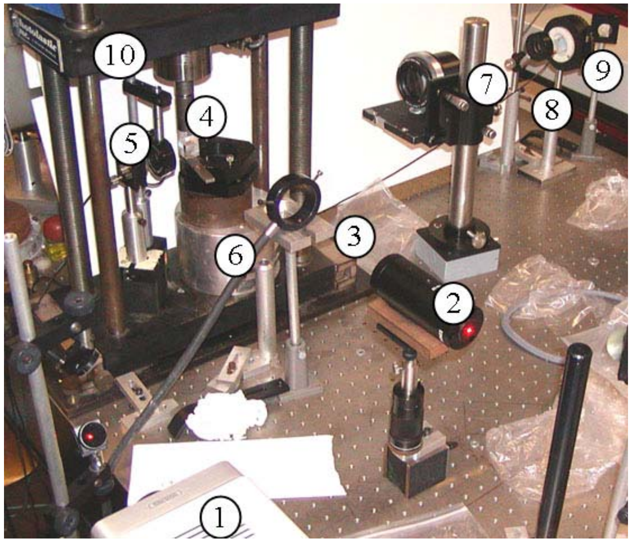

- **–Prototype on optical table**
- –Perform preliminary indentation tests

1. HeNe laser, 2. Beam expander, 3. Ring light source, 4. Indenter head, 5. $\lambda/4$ waveplate and reference mirror, 6. Specimen holder, 7. Imaging lens, 8. LCVR, 9. Polarizer, 10. Loading system

Application of TIM Technique: E and stress-strain evaluation

Loading: Fringe pattern, wrapped phase and contact radius

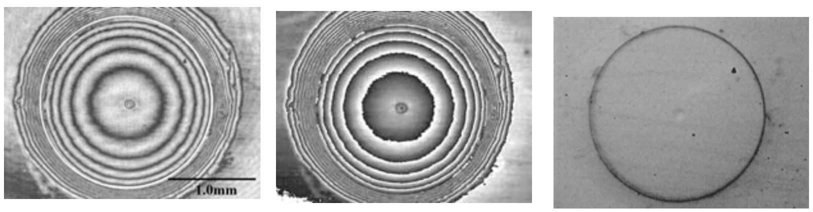

Unloading: Fringe pattern, wrapped phase and contact radius

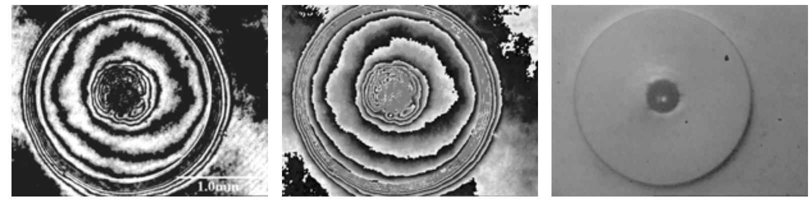

Loading: Fringe pattern, wrapped phase and contact radius

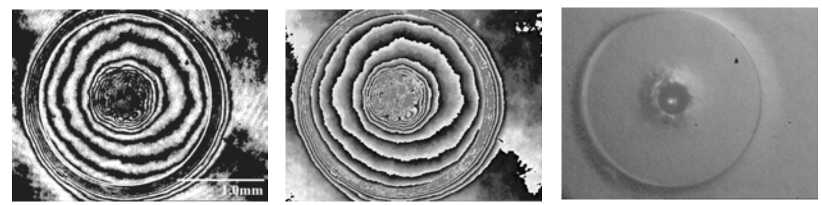

Unloading: Fringe pattern, wrapped phase and contact radius

	IN783 (E = 177.3GPa)	
	Average	Max. Error
Spherical Indentation	**174.5GPa**	**≤ 5%**

	Al 6061-T0 (E = 69GPa)	
	Average	Max Error
Spherical Indentation	**70.3GPa**	**≤ 4%**

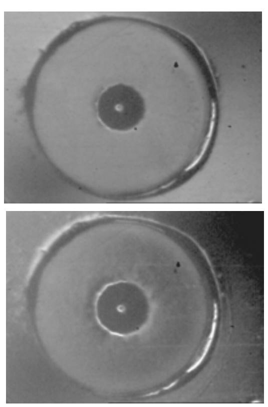

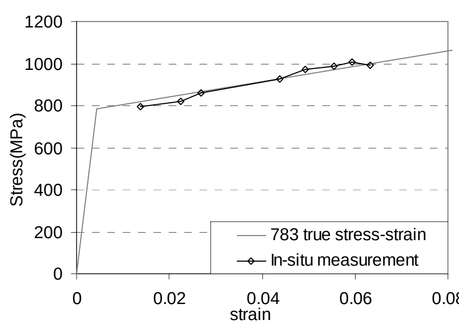

IN783

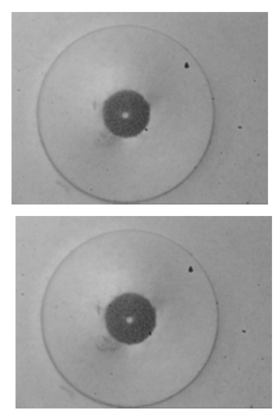

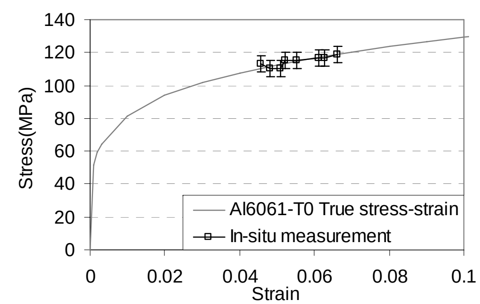

Al 6061-T0

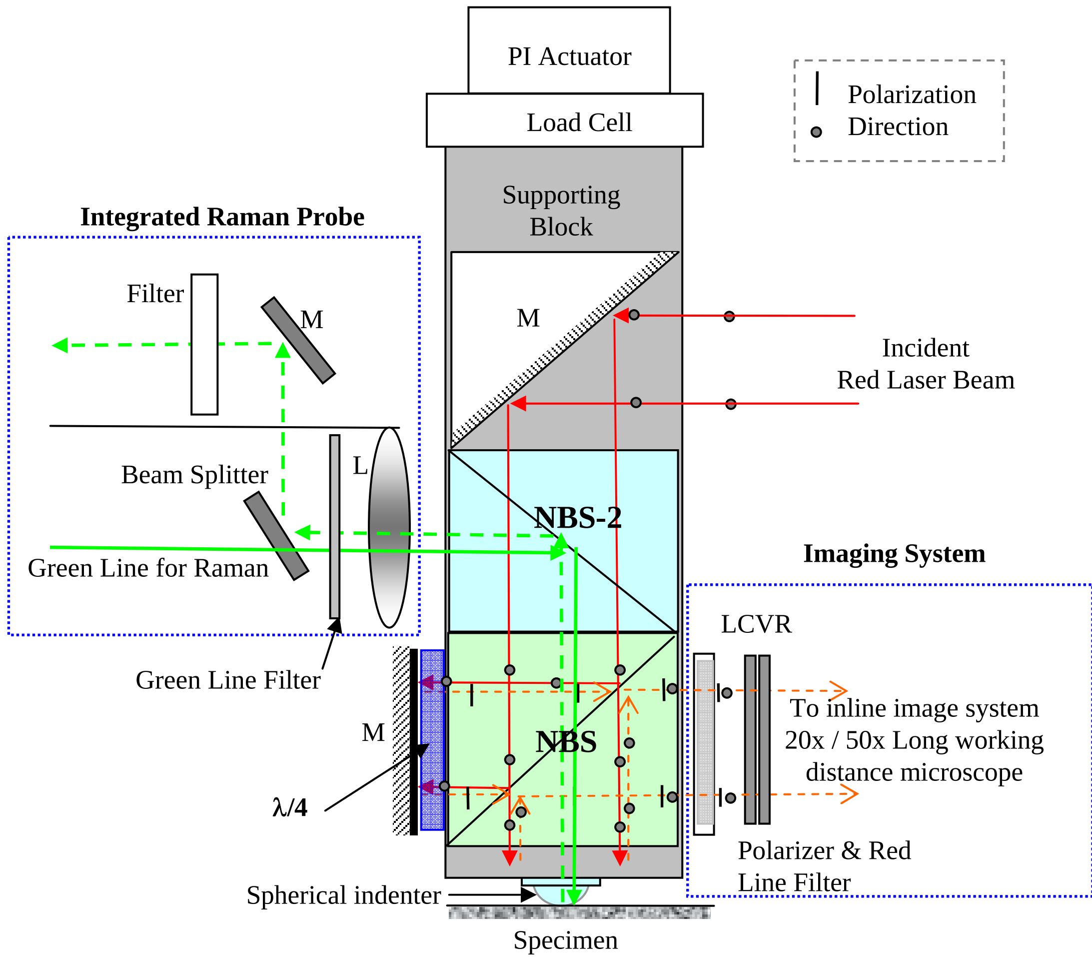
PI Actuator
Load Cell
Supporting Block
Polarization Direction
Integrated Raman Probe
Filter
M
Beam Splitter
L
Green Line for Raman
M
Incident Red Laser Beam
NBS-2
Imaging System
LCVR
Green Line Filter
M
NBS
To inline image system 20x / 50x Long working distance microscope
λ/4
Polarizer & Red Line Filter
Spherical indenter
Specimen

West Virginia University

Gen II: Simplified Transparent Indenter Measurement System

- No laser interferometry, white light illumination only.
- Young’s modulus without dedicated displacement sensor
- Laboratory table top setup and Portable setup

Principle

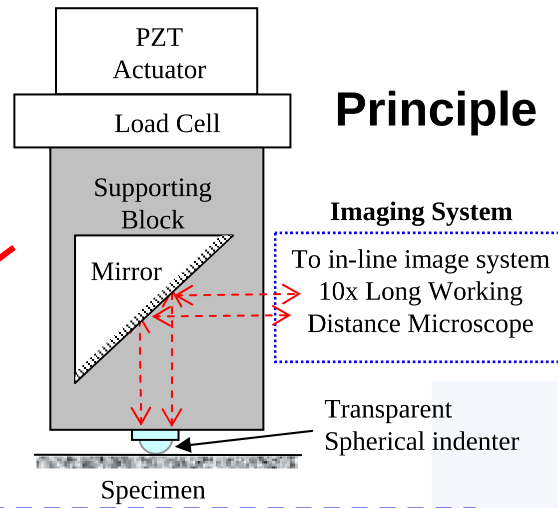

Table top setup


Governing Equations

$$\left(\frac{dh_{PZT}}{dp}\right) = \left(\frac{1}{E_r}\right)\left(\frac{\sqrt{\pi}}{2}\frac{1}{\sqrt{A}}\right) + S_s$$

$$y = ax + b$$

$$x = \frac{\sqrt{\pi}}{2}\frac{1}{\sqrt{A}} \qquad a = \frac{1}{E_r}$$

$$y = \frac{dh_{PZT}}{dp} \qquad b = S_s$$

Portable setup

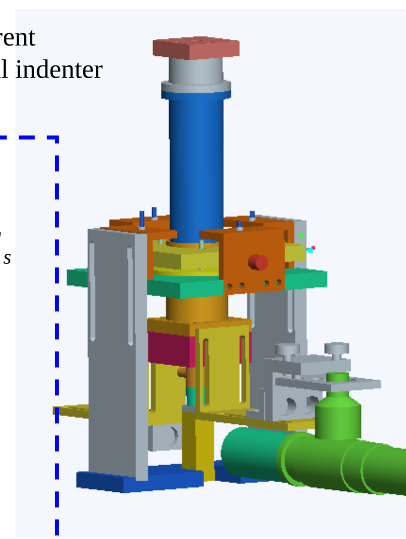
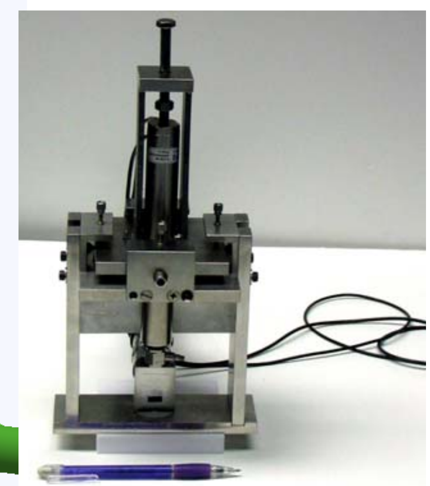

Instrumented Indentation Technique

- Young's modulus (E)

$$\frac{dP}{dh} = \frac{2}{\sqrt{\pi}} E_r \sqrt{A}$$ (Spherical indentation)

Where *Er* is the reduced Young's modulus,

$$\frac{1}{E_r} = \frac{1-\nu^2}{E} + \frac{1-\nu_0^2}{E_0}$$

(M.F. Doerner et al, 1986)

(Oliver and Pharr, 1992

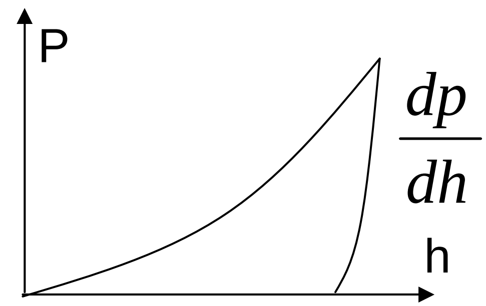

P-h curve from load-depth sensing indentation test

A: contact region (derived from dp/dh or direct measurement)

- Post-yielding stress-strain data
  - Tabor's empirical relation:
    d : contact diameter, D *:* indenter diameter, *Pm:* mean pressure *C:* constraint factor.
  - Constraint factor C is strain hardening depended

$$\varepsilon = 0.2\frac{d}{D}$$

$$\sigma = \frac{P_m}{C} \qquad P_m = \frac{Load}{\pi a^2}$$

Multi-partial Unloading Procedure for E

$$\left.\frac{dh_s}{dP}\right|_1 = \frac{\sqrt{\pi}}{2}\frac{1}{\sqrt{A_1}}\frac{1}{E_r} + S_s$$

$$\left.\frac{dh_s}{dP}\right|_2 = \frac{\sqrt{\pi}}{2}\frac{1}{\sqrt{A_2}}\frac{1}{E_r} + S_s$$

Double-partial unloading

$$\left.\frac{dh_s}{dP}\right|_1 - \left.\frac{dh_s}{dP}\right|_2 = \frac{\sqrt{\pi}}{2}\frac{1}{E_r}\left(\frac{1}{\sqrt{A_1}} - \frac{1}{\sqrt{A_2}}\right)$$

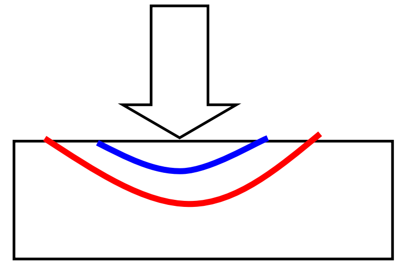

Multiple-partial unloading

$$\left(\frac{dh_{PZT}}{dp}\right) = \left(\frac{1}{E_r}\right)\left(\frac{\sqrt{\pi}}{2}\frac{1}{\sqrt{A}}\right) + S_s$$

$$y = ax + b$$

$$x = \frac{\sqrt{\pi}}{2}\frac{1}{\sqrt{A}}$$

$$y = \frac{dh_{PZT}}{dp}$$

$$a = \frac{1}{E_r}$$

$$b = S_s$$

$$E = \frac{1 - v^2}{\frac{1}{E_r} - \frac{1 - v_0^2}{E_0}}$$

IN783

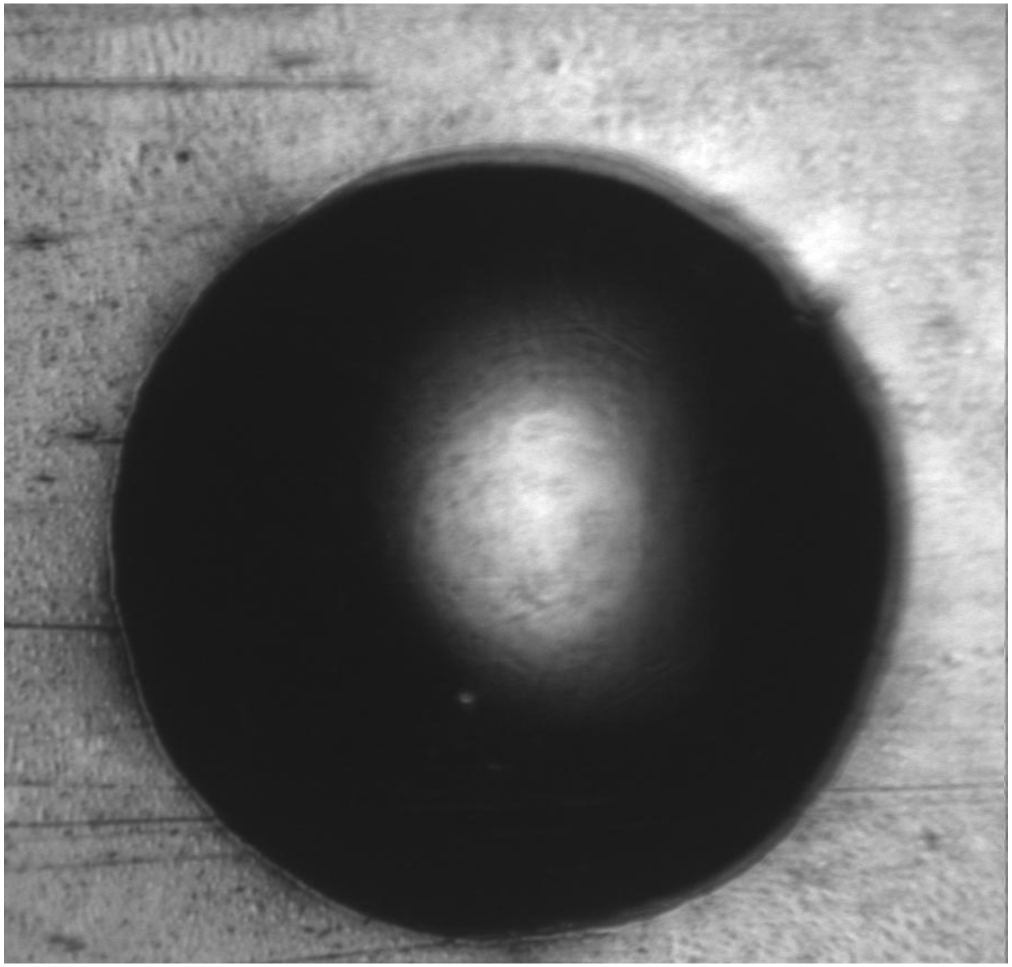

IN783

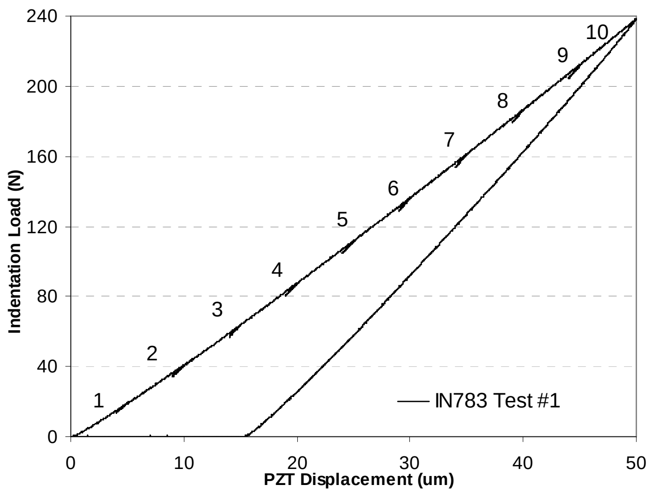

(a) Load-displacement curve

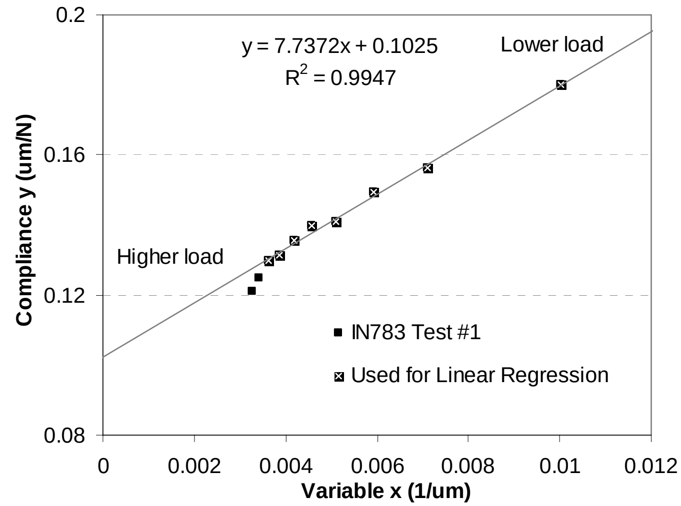

(c) Plot for Young's modulus evaluation, E=177.9±6.1GPa

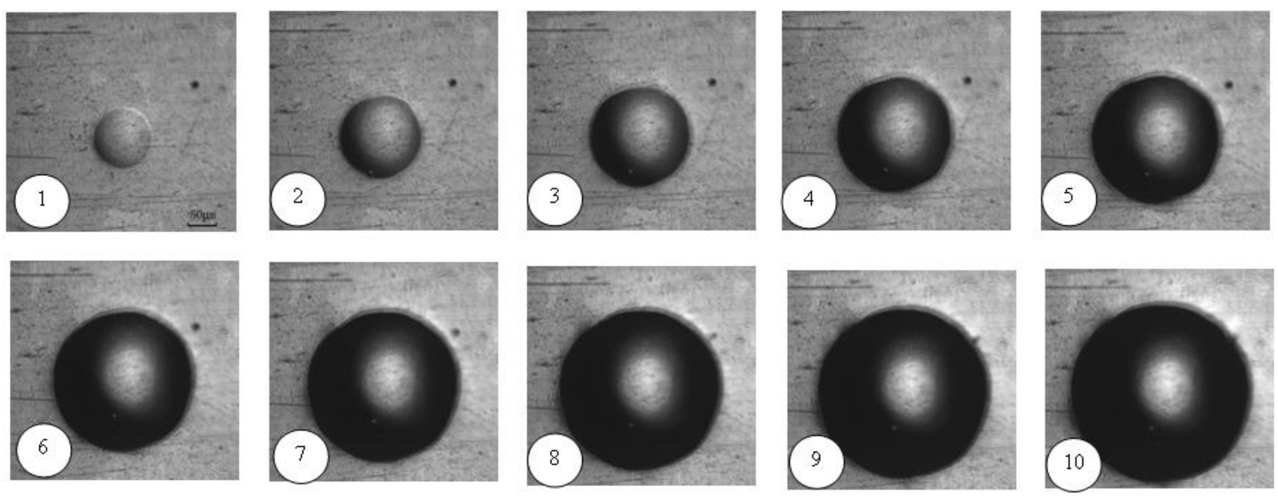

(b) Visualization of indented surface, Field of view for each image: 395um x 377um

Indentation Method for Stress-Strain Evaluation

- Initial multiple-partial unloadings for Young's modulus determination and followed by discrete loadings for post-yielding stress/strain data based on Tabor's equations

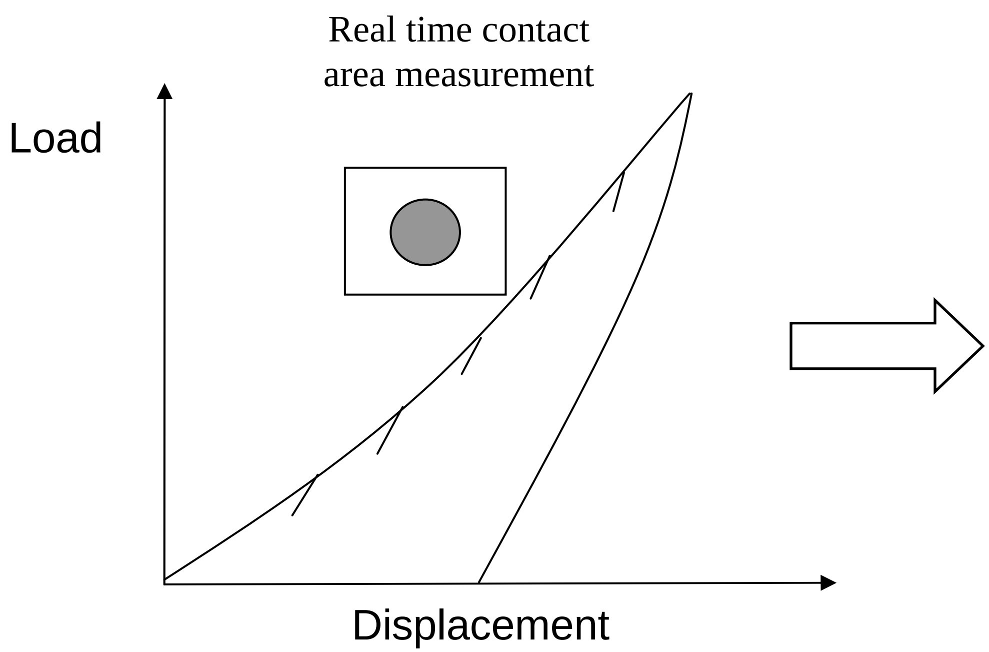

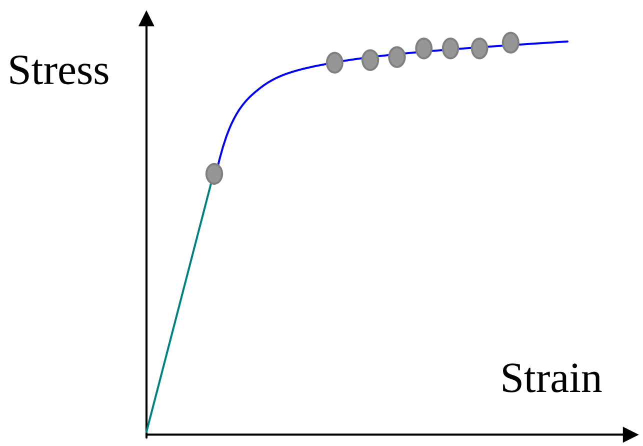

ORNL Cast Re-(26-30) Cr wt% Alloy

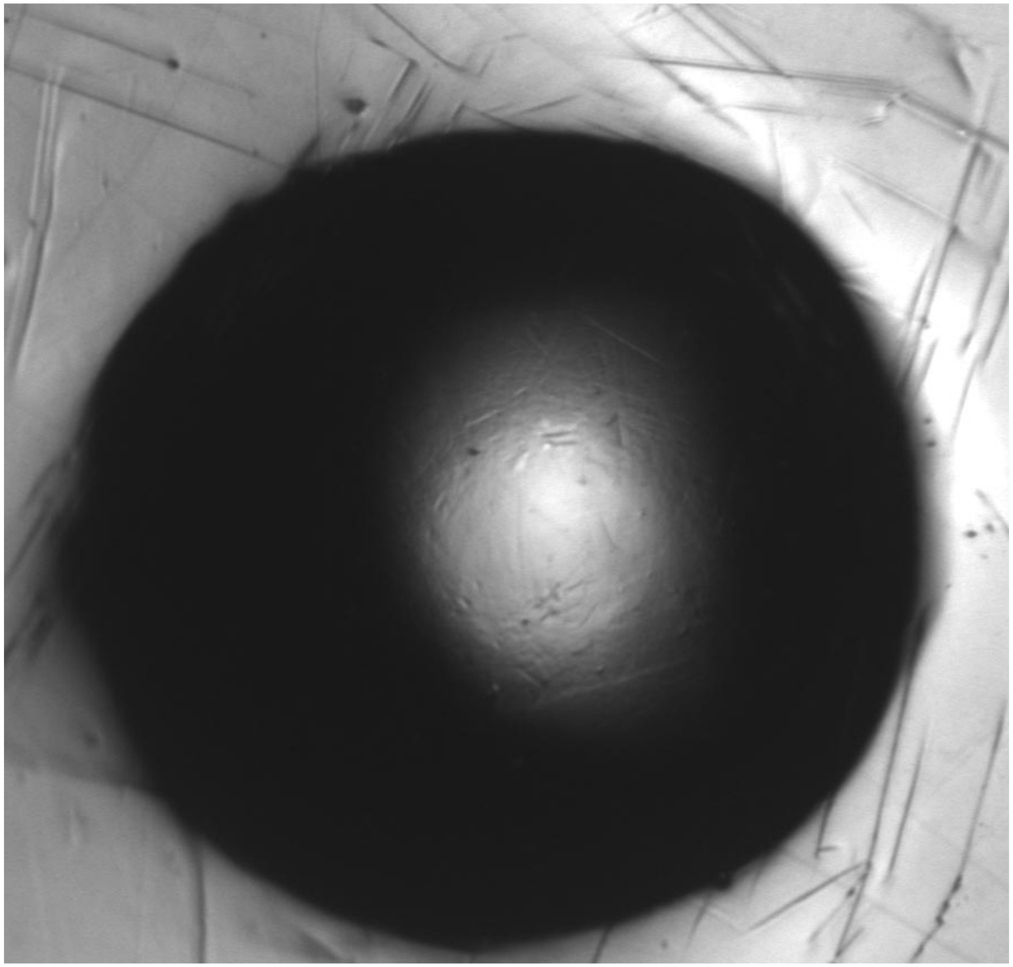

Application: ORNL Cast Re-(26-30) Cr wt% Alloy

- Initial multiple-partial unloadings for Young's modulus determination and followed by discrete loadings for post-yielding stress/strain data based on Tabor's equations.

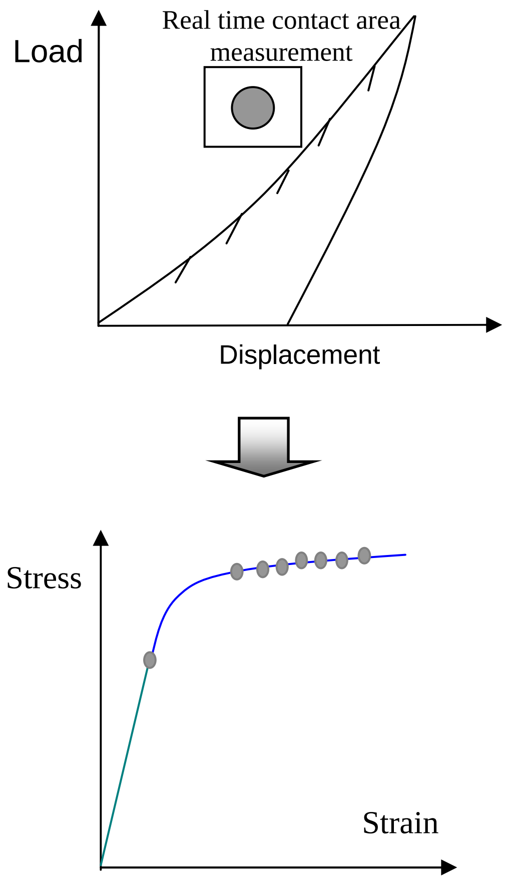

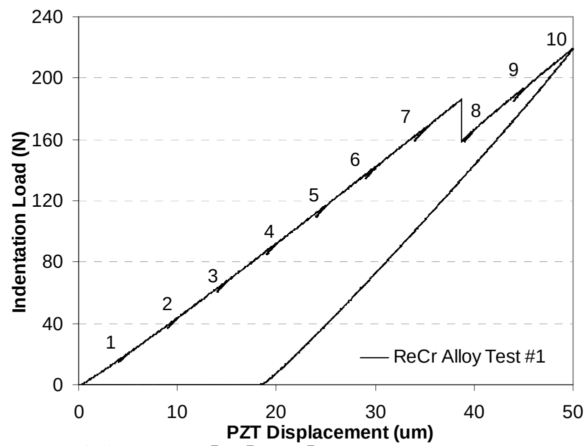

(a) Load-displacement curve

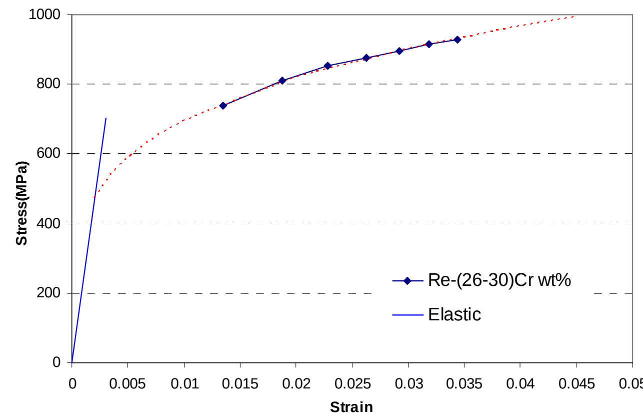

(c) Stress-strain curve, E=234GPa

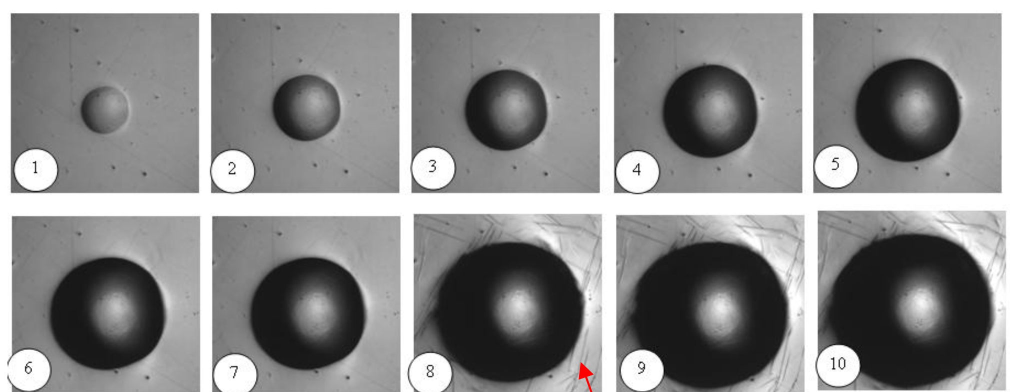

Showing formation of slip lines

(b) Visualization of indented surface, Field of view for each image: 395um x 377um

Gen III: Multi-Partial Unloading Indentation Technique

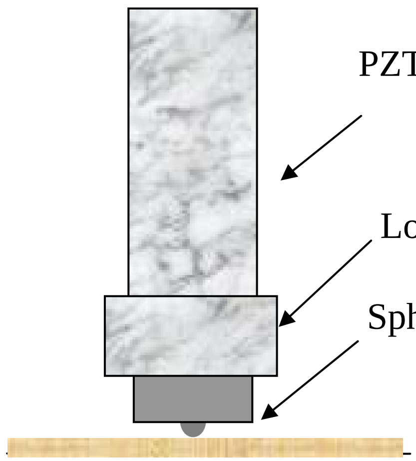

Load-depth sensing indentation system without imaging

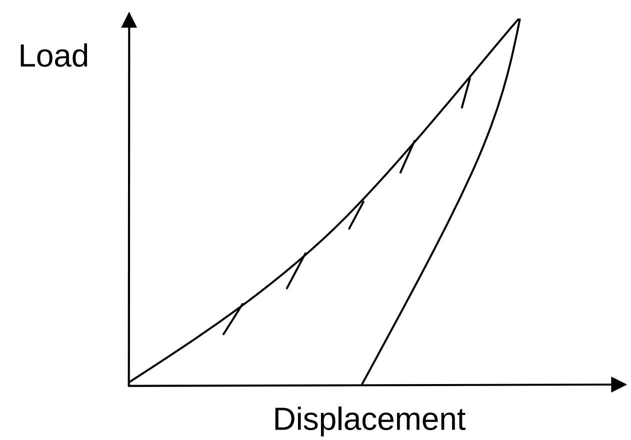

Multi-partial unloading indentation technique

Governing Equations

$$\frac{dh}{dp} = C \times \frac{1}{p^{1/3}} + C_s$$

$$C = \left(6RE_r^2\right)^{-1/3}$$

Applications:

- Young's modulus evaluation
- Stress-strain curve assessment
- Indentation creep evaluation
- Other application: TBC investigation

Application: IN783 (Using Gen III indentation technique)

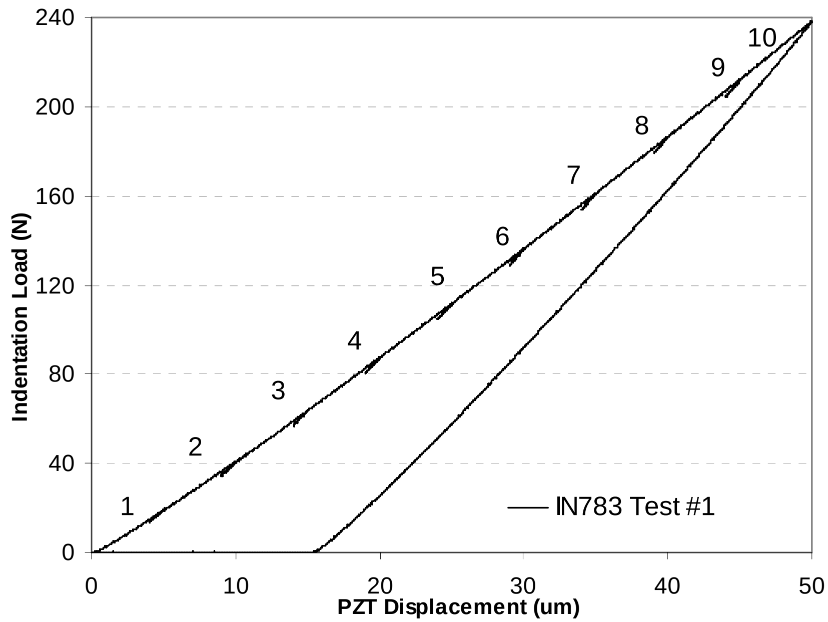

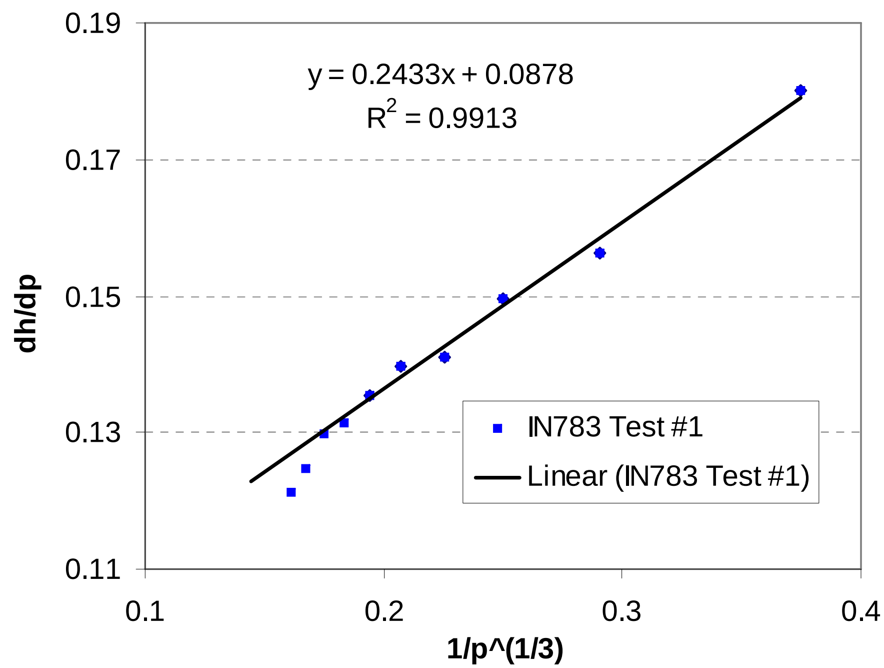

Using only the load-displacement curve, Young's modulus was determined from five indentation tests (168.4GPa ± 5.1GPa)

Application: Molybdenum Alloy

Typical load-displacement curve, ORNL #678, #696, #697, #698 alloys

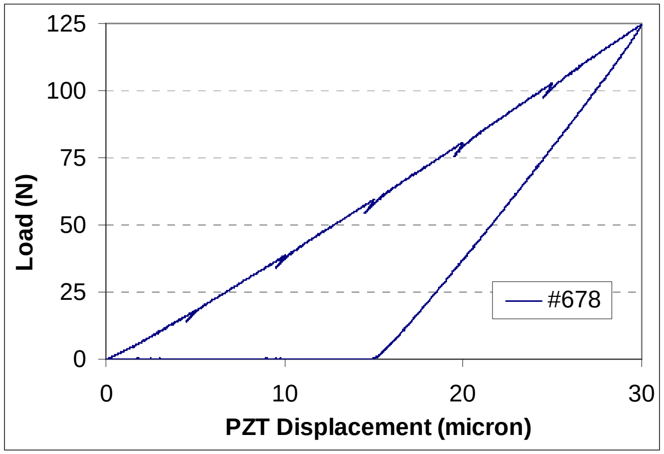

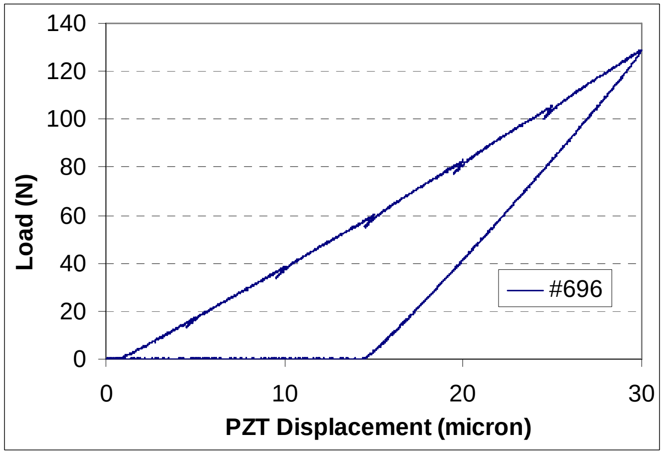

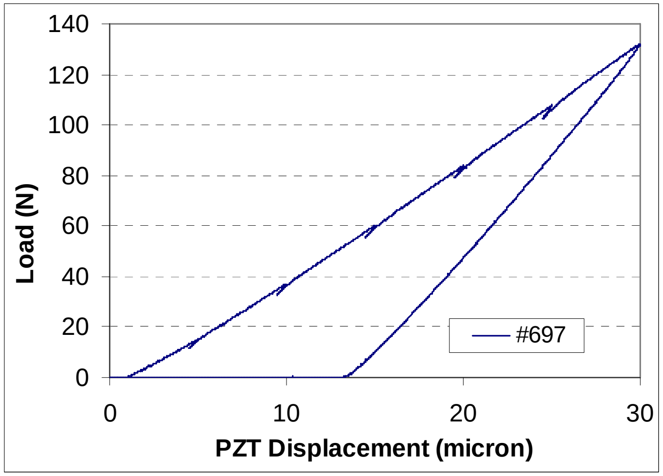

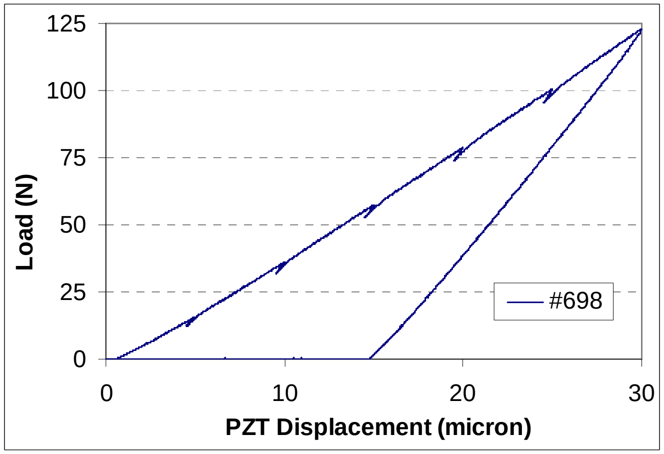

Application: Molybdenum Alloy

Typical load-displacement curve, WVU Mo-MgO, Mo-$MgAl_2O_4$, Mo-TiO_2 alloys

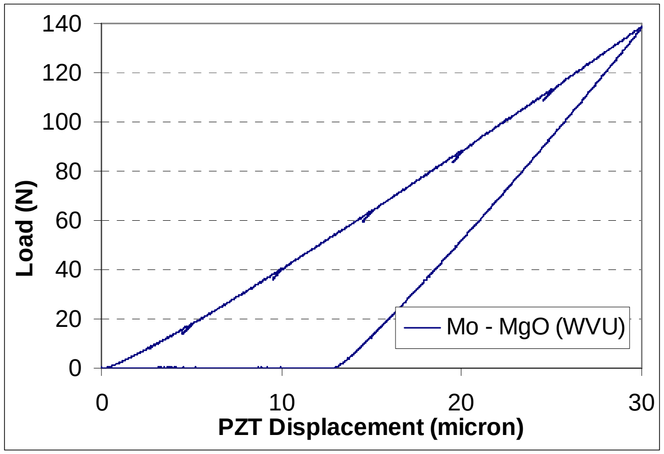

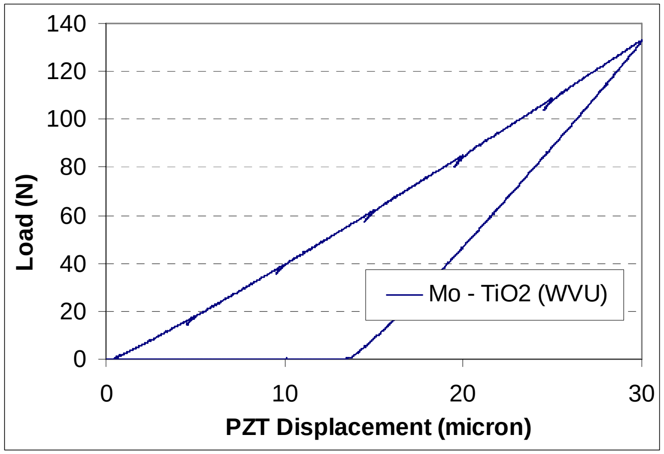

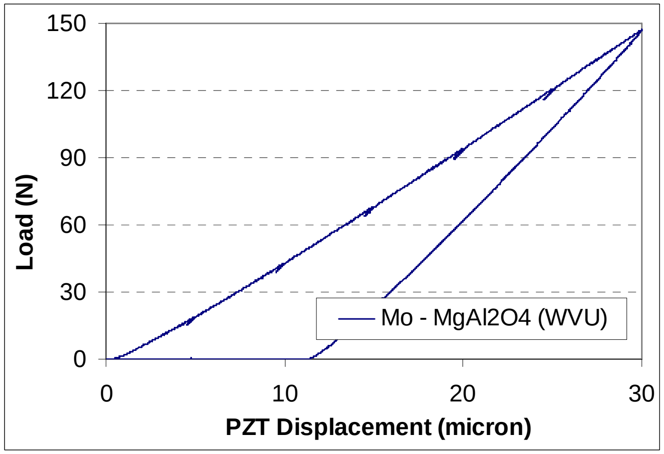

Summary: Young's Modulus Measurement

Material	Young's modulus (GPa)
Cast Re-(26-30) Cr wt%	234
#678, Mo-3.4wt%$MgAl_2O_4$	229
#696, Mo-3.0wt%$MgAl_2O_4$	200
#697, Mo-6.0wt%$MgAl_2O_4$	192 (Tensile test : 189)
#698, Mo-3wt%MgO	211
Mo-MgO (WVU)	254
Mo-MgAl2O4 (WVU)	202
Mo-TiO2 (WVU)	226

(Averaged value from five indentation tests, typical)

- Ductile/Brittle assessment using indentation technique
  - Indentation-induced surface cracking
  - Surface profile/slip lines/shear bands

Material surface condition evaluation Mo alloys with spinel particles

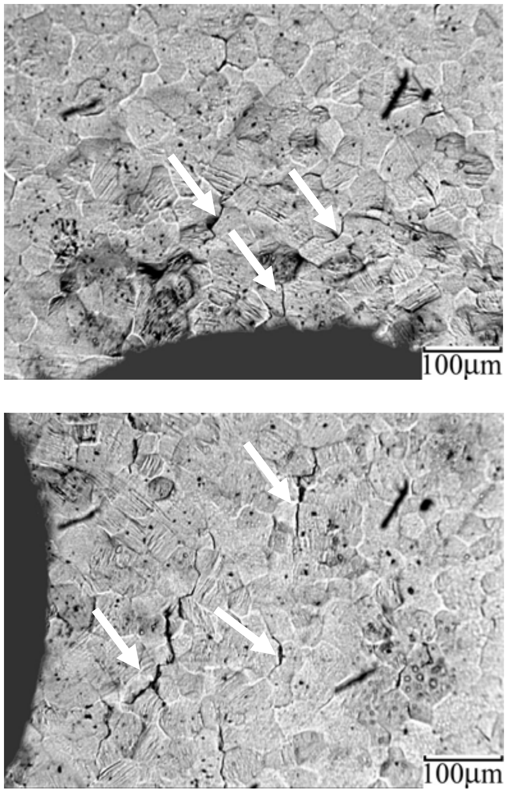

#695, brittle, indentation load 1500N, cracks are observed

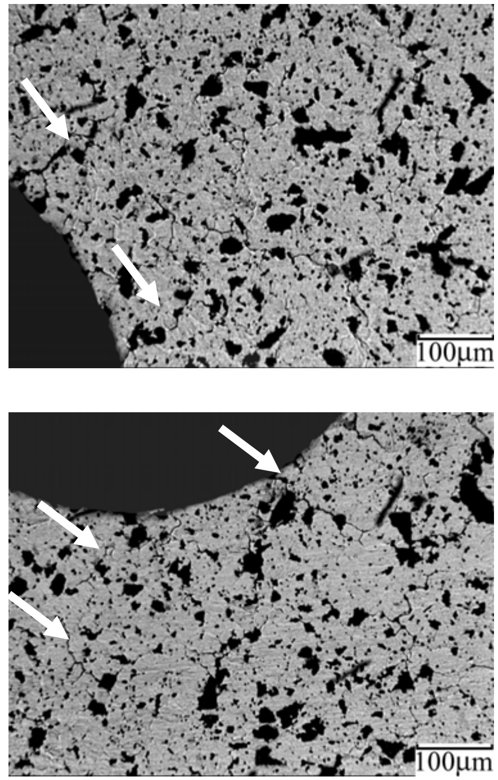

#697, brittle, indentation load 1000N, cracks are observed

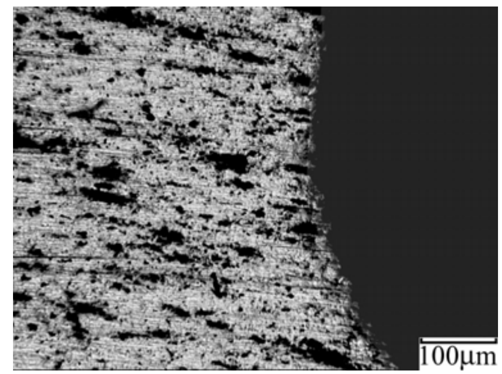

#678, Ductile, indentation 2000N, no cracks were observed

After spherical indentation, surface was evaluated under

Optical Microscope, 10x. Cracks are marked with arrows

Material surface condition evaluation Mo alloys with spinel particles

SEM observation at 2000x

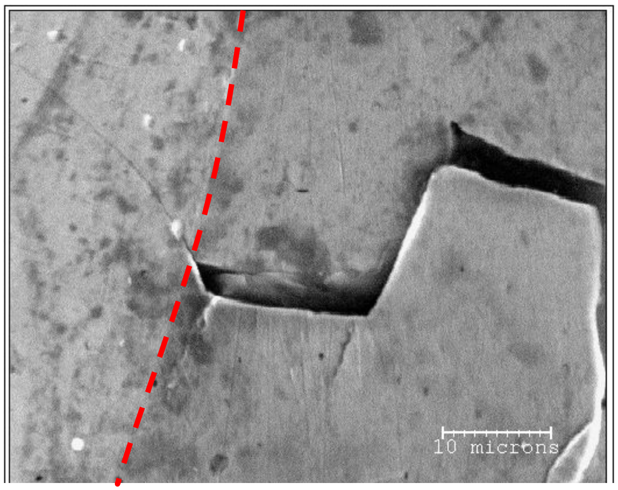

#695, brittle, indentation load 1500N, cracks are observed

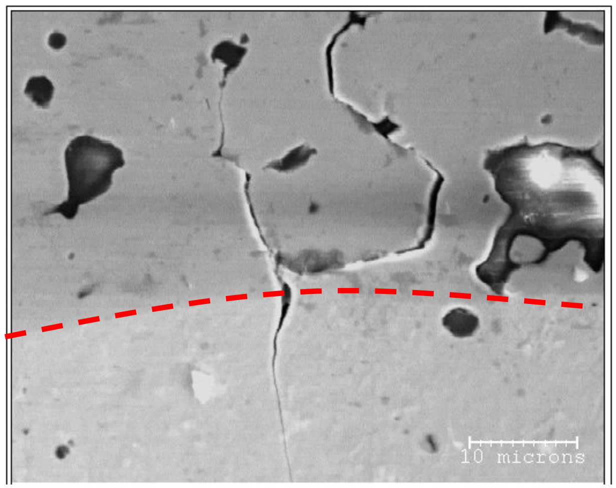

#697, brittle, indentation load 1000N, cracks are observed

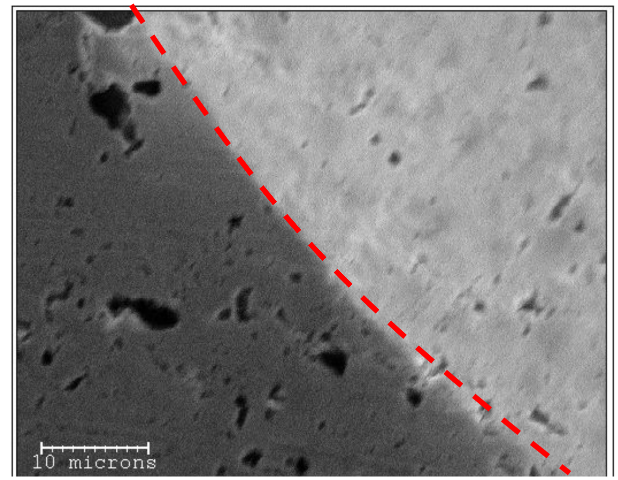

#678, Ductile, indentation load 2000N, no cracks were observed

Note: Dashed lines are indent boundaries

#696, Mo-3.0wt%$MgAl_2O_4$

- 400N indentation, cracking

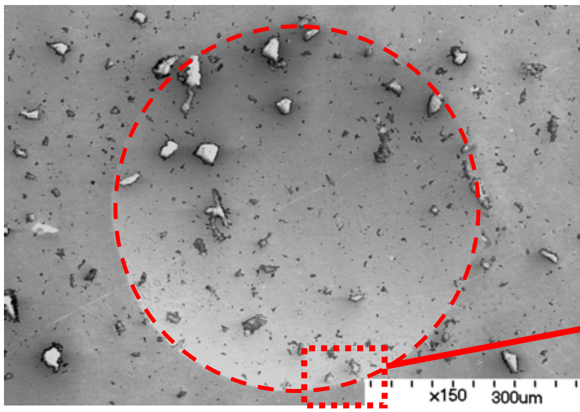

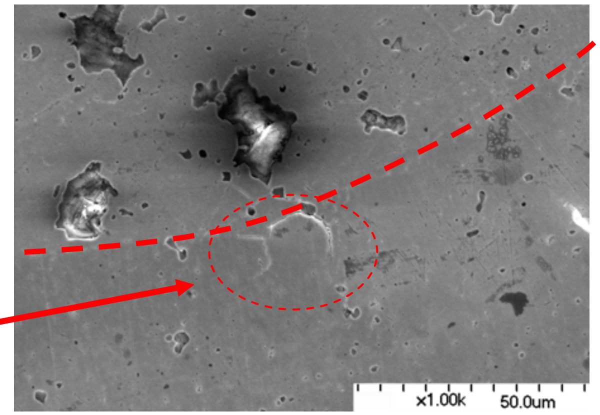

- 1000N indentation, cracking

1000N indentation with 1.6mm WC indenter

(Image size: 321μm×240μm)

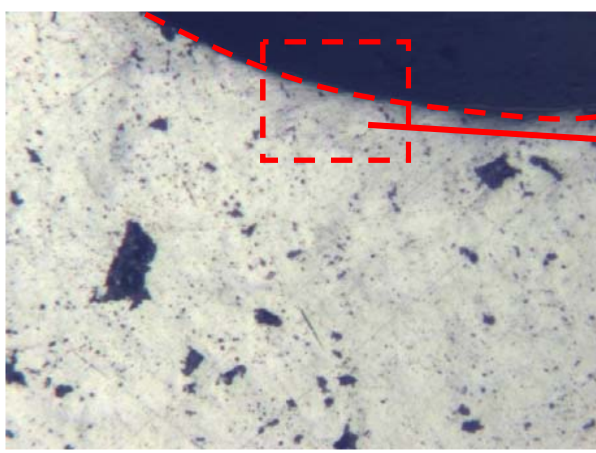

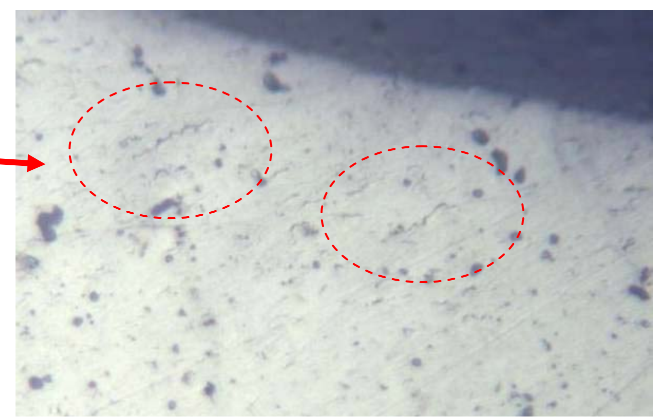

#698, Mo-3wt%MgO

- 400N indentation, cracking

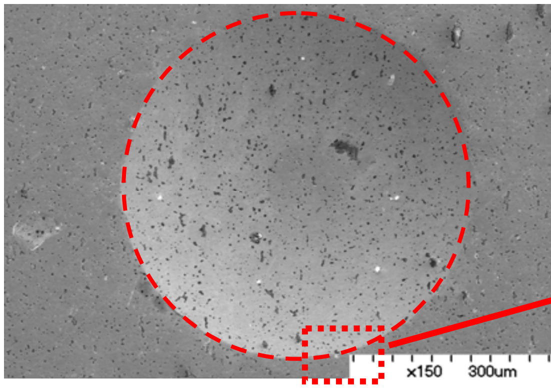

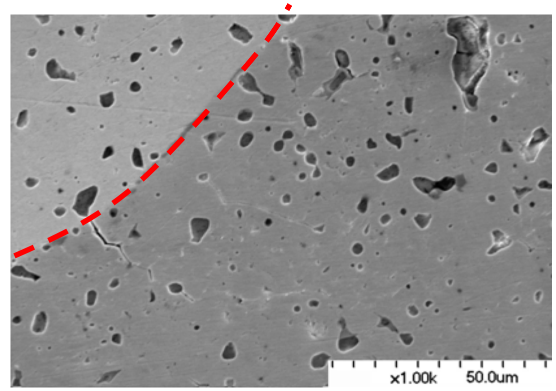

- 1000N indentation, cracking

1000N indentation with 1.6mm WC indenter

(Image size: 321μm×240μm)

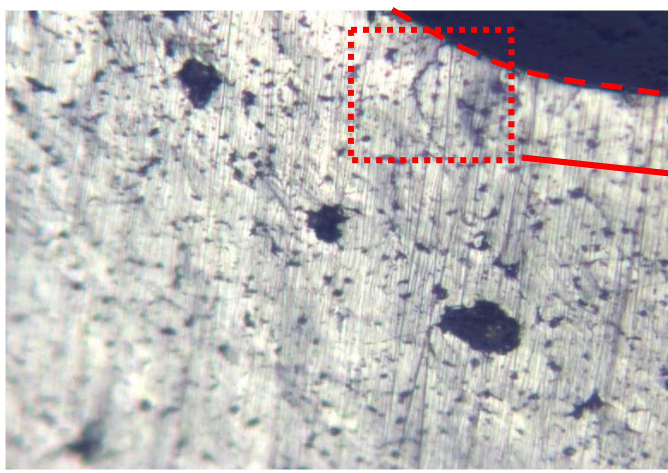

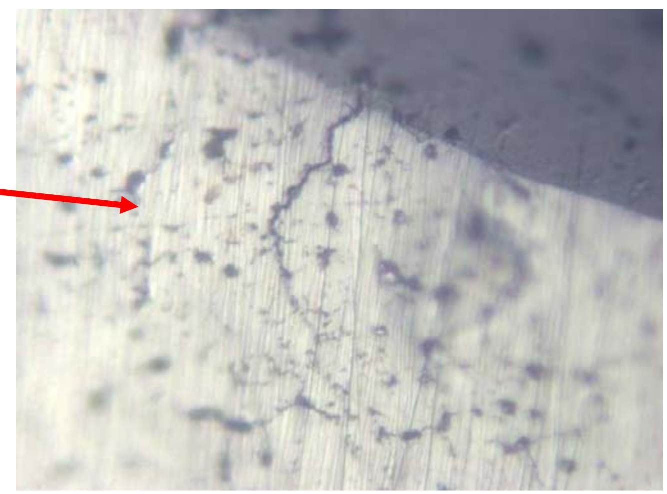

Mo-TiO_2 (WVU)

- 400N indentation, cracking

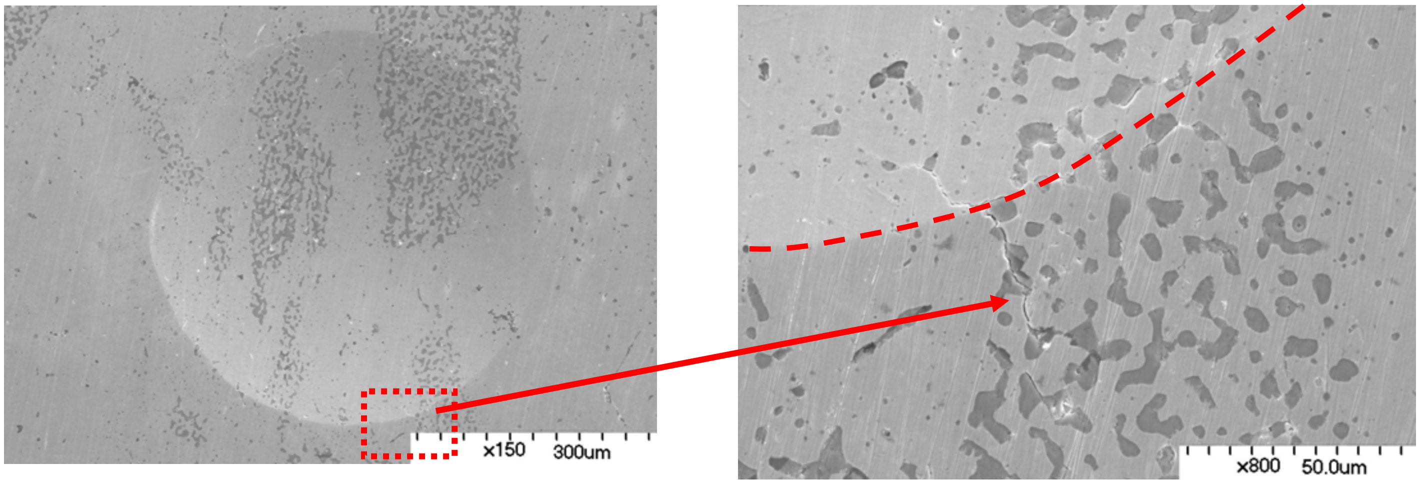

- Vickers hardness

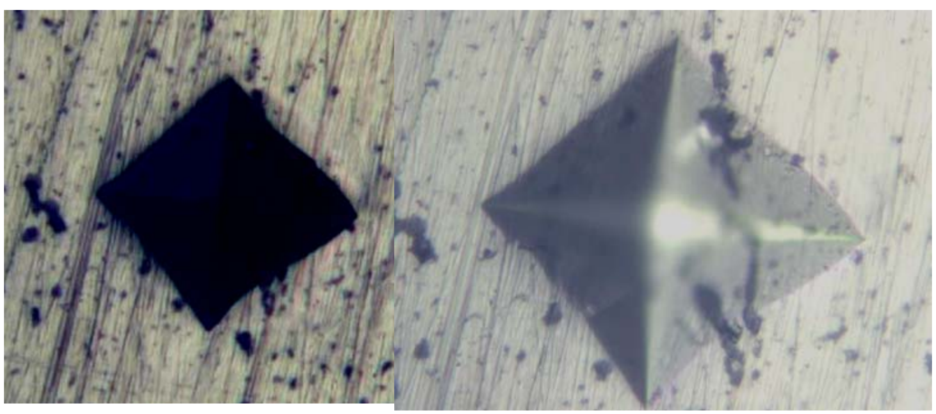

223HV, 1kg, 30s

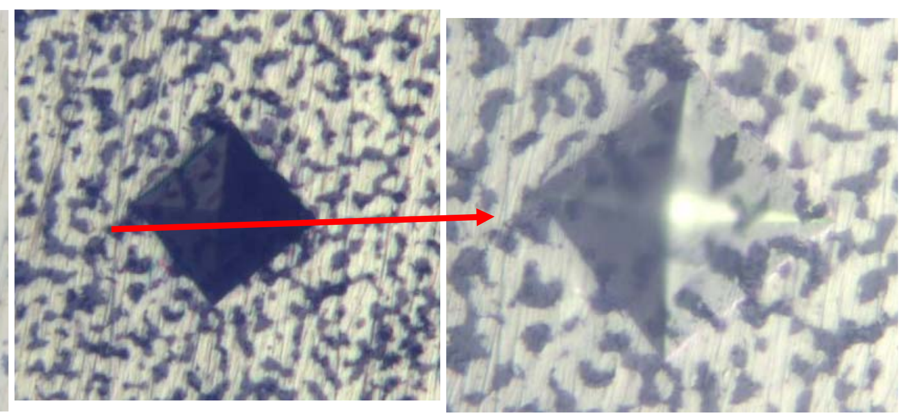

353HV, 1kg, 30s

Mo-MgO (WVU)

- 400N indentation, cracking

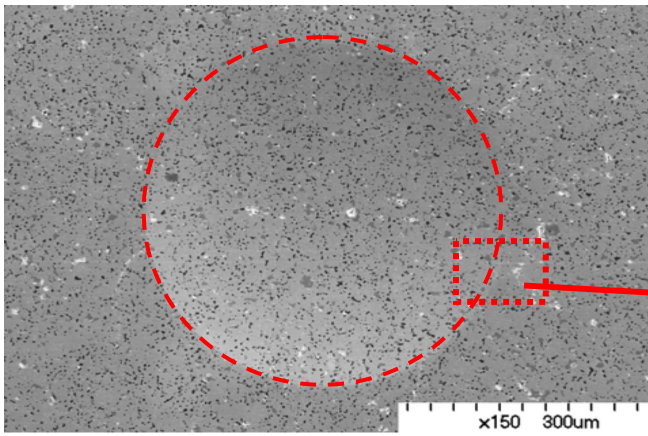

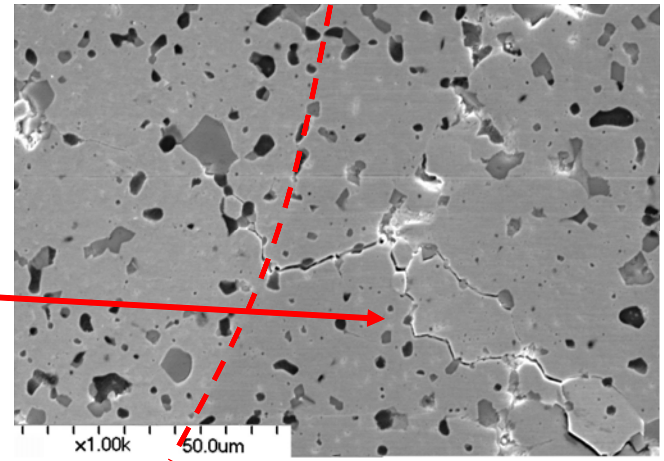

- Vickers hardness, 249HV, 1kg, 30s

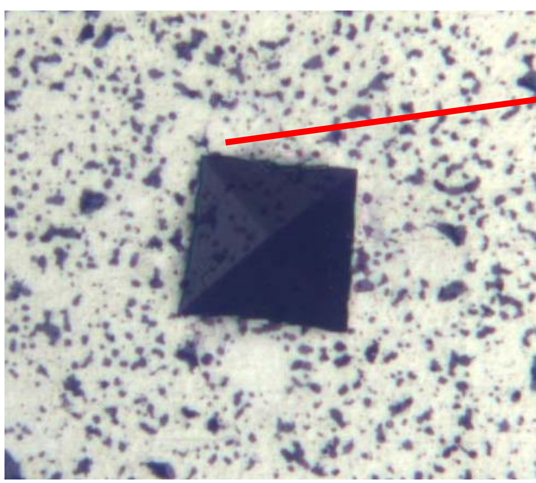

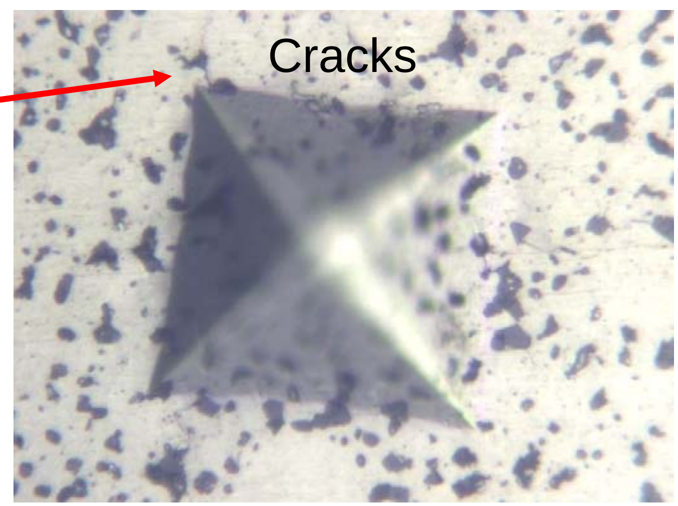

Mo-$MgAl_2O_4$ (WVU)

- 400N indentation, no cracks in MgAl2O4 uniformly distributed region

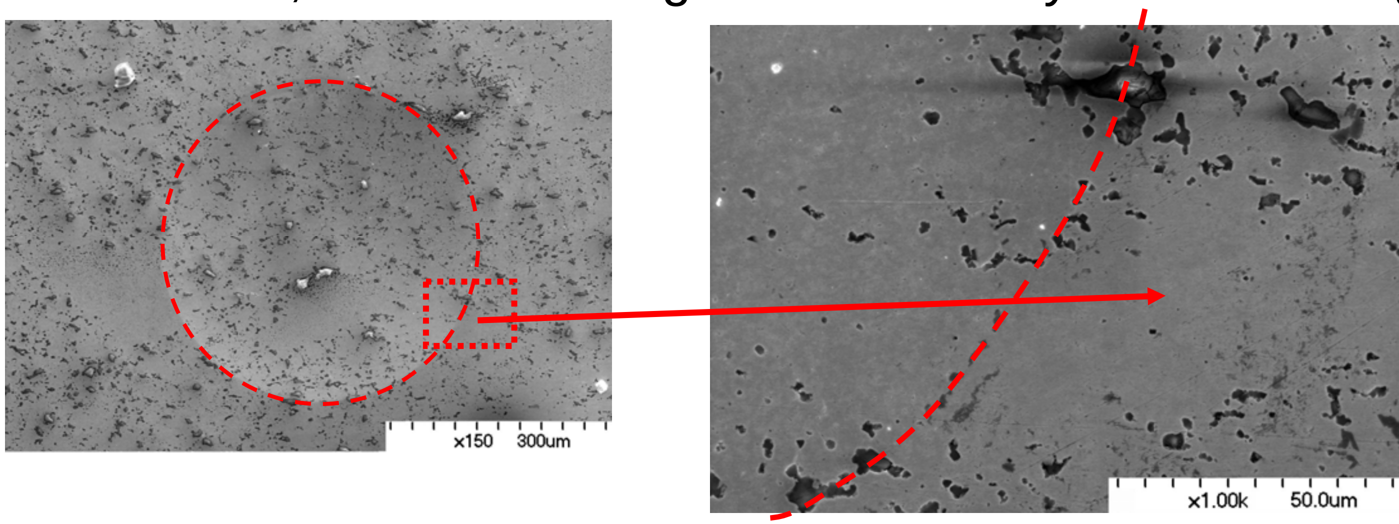

- Vickers hardness (plastic flow observed)

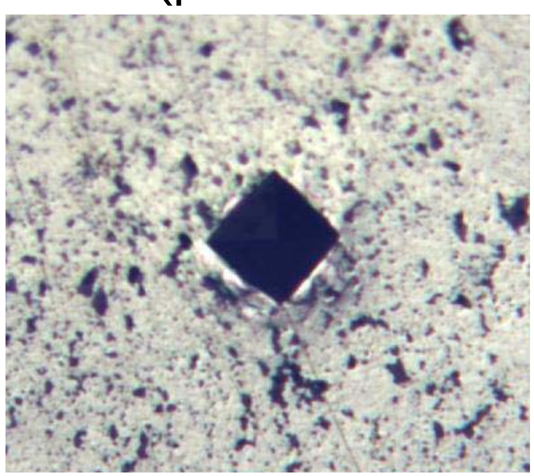

276HV, 1kg, 30s

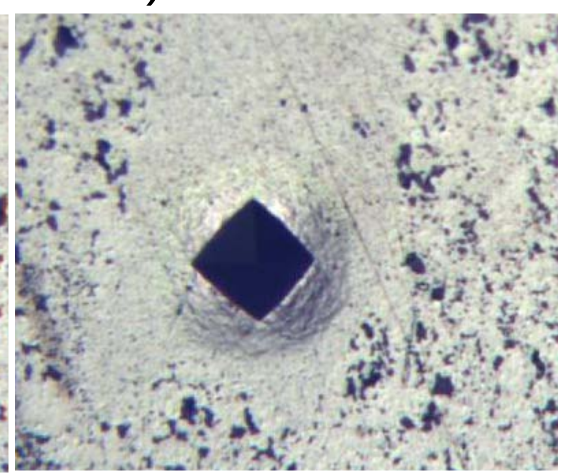

344HV, 1kg, 30s

Conclusion:

- (contrary to Cr alloys) Mo with $MgAl_2O_4$ spinel has better room-temperature ductility improvement than Mo with MgO

- Mo with nano-size $MgAl_2O_4$ spinel showed promising result, however, optimized processing condition needs to be developed for uniform oxide dispersion

- Developed a micro-indentation technique for in-situ mechanical property measurement

Planned Research:

Indentation Test at Elevated Temperature

Goal:

- Stress-strain relation evaluation at elevated temperatures up to 1200 C

- Indentation creep test at elevated temperatures

High Temperature Indentation Using Multi-Partial Unloading Technique

(Less difficult to implement)

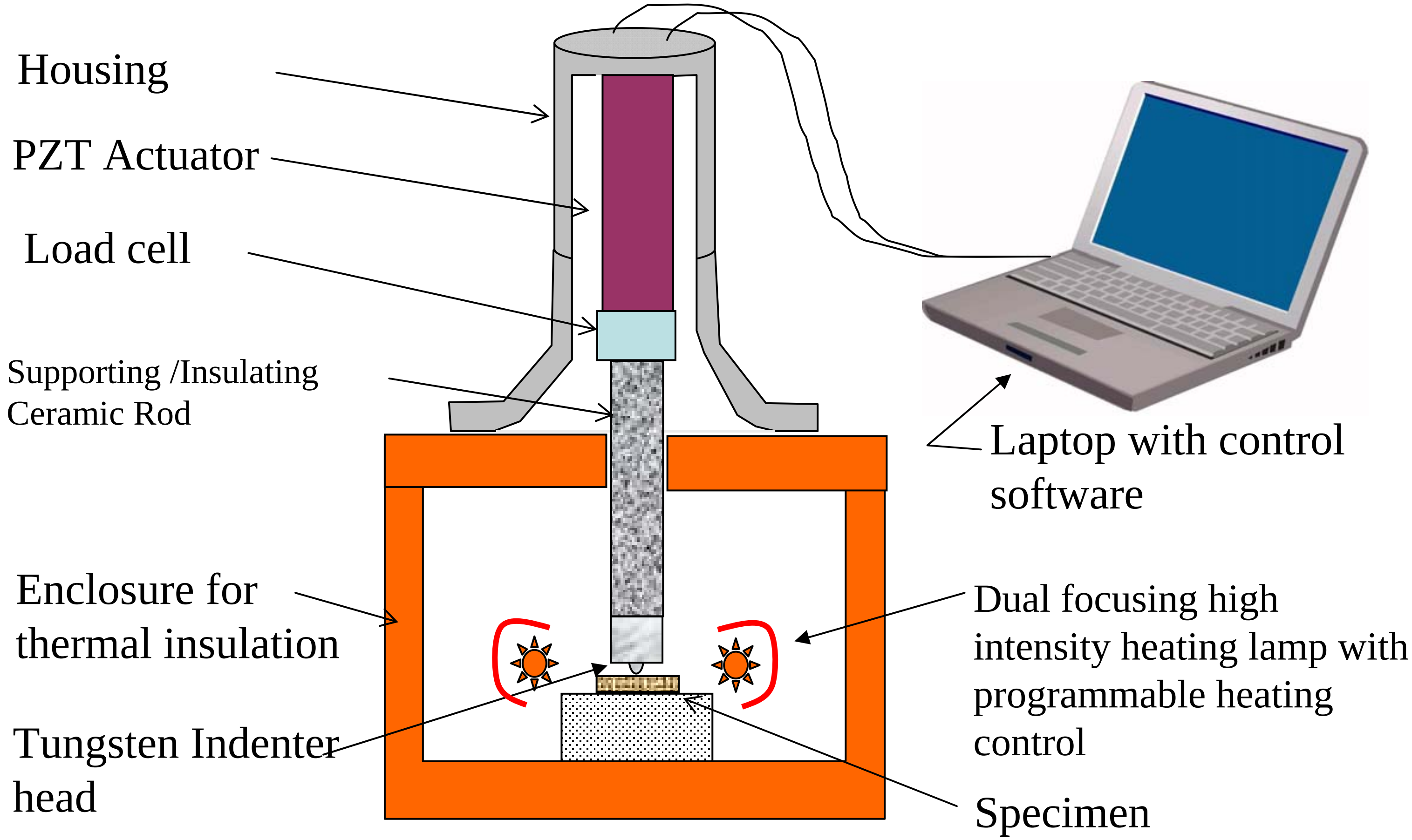

- Based on Gen III multi-partial unloading indentation technique
- Compact design (size of the indenter: 2 in diameter 12 in long)
- Data processing is less complicated

Thank You !

XRD pattern of as-prepared and hot-pressed MgO0.05Mo0.95 samples. Note the shift of the lines to higher angles in the hot-pressed sample.

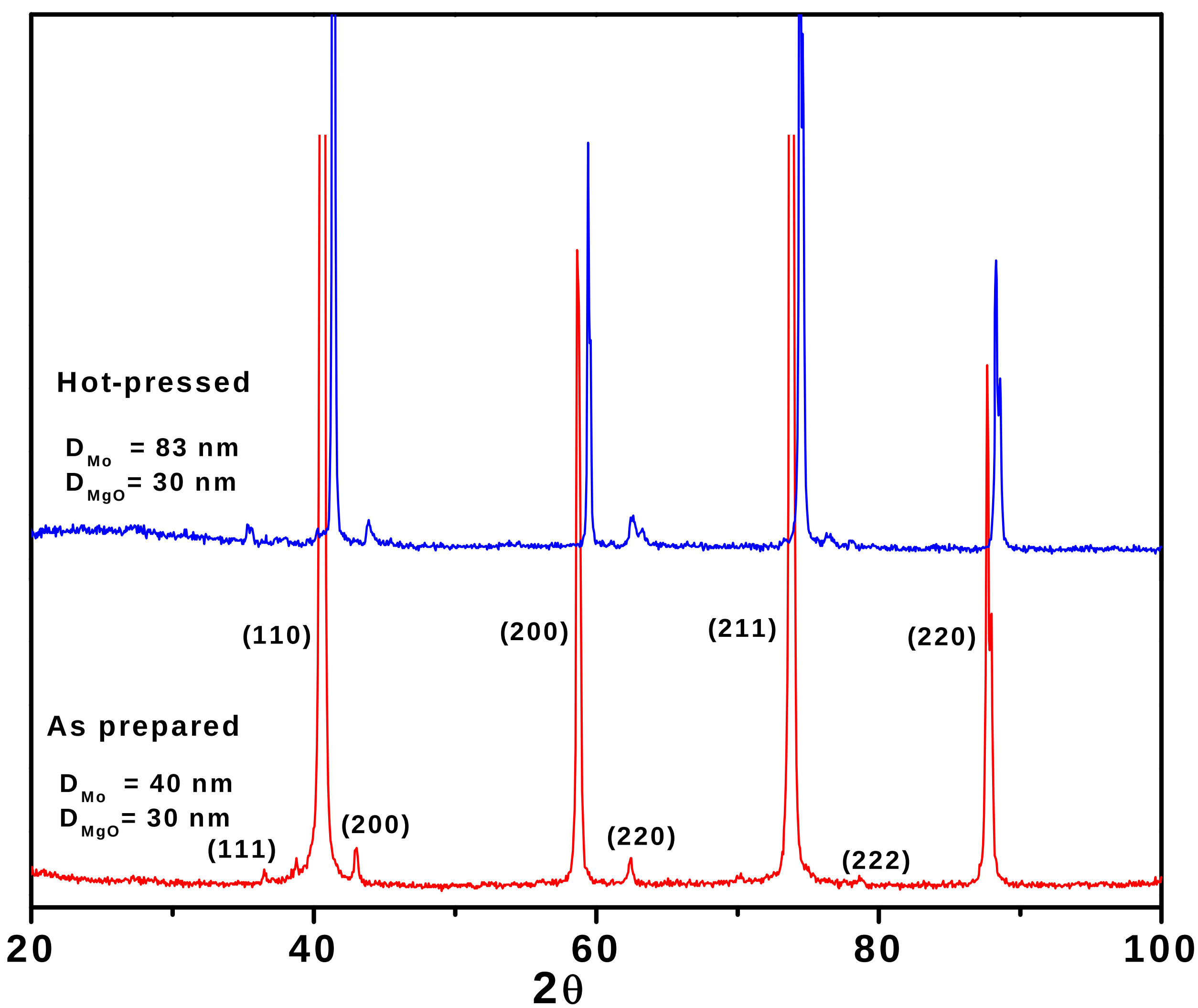

Particle size and strain values of the samples calculated from the modified Scherrer equation

Sample	Component	Particle size (D) nm	Strain (η) ×10^{-3}
Mo (as-received)	Mo	65	3.4
MgO (as-received)	MgO	20	0.9
$MgO_{0.05}Mo_{0.95}$ (as-prepared)	Mo	43	2.7
	MgO	30	
$MgO_{0.05}Mo_{0.95}$ (ball-milled)	Mo	12	11.5
	MgO	30	
$MgO_{0.05}Mo_{0.95}$ (hot-pressed)	Mo	83	6.1
	MgO	30	

#695 Mo, Vickers hardness

- 174HV, 1kg, 30s

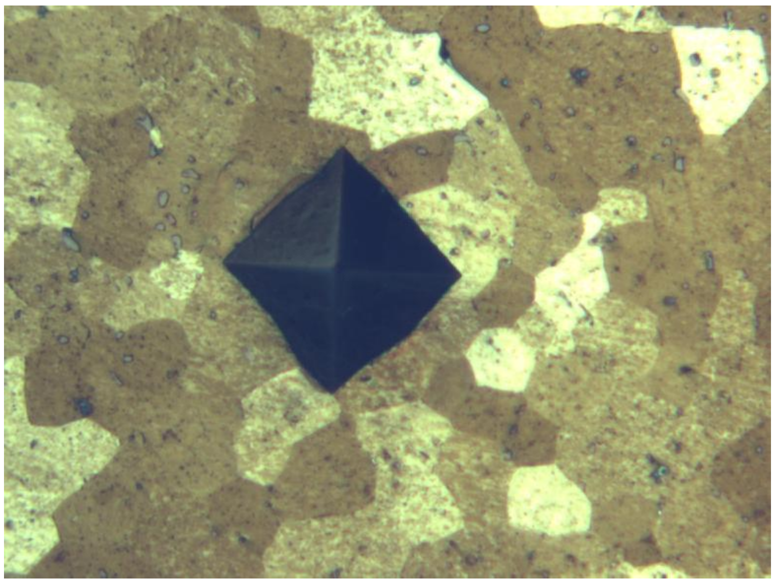

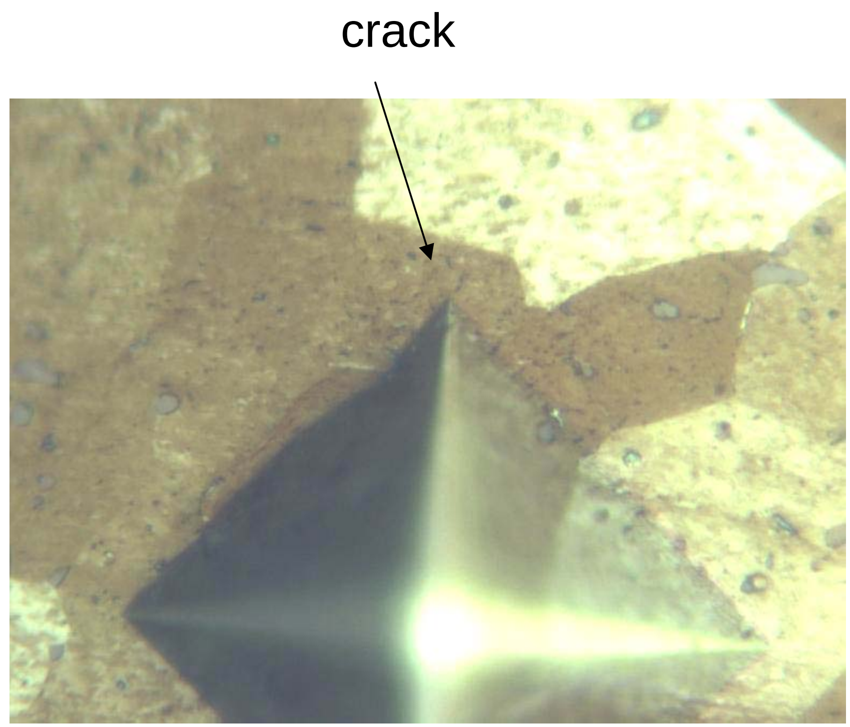

#697, Mo-6.0wt%$MgAl_2O_4$, Vickers Hardness

234HV, 1Kg, 30S

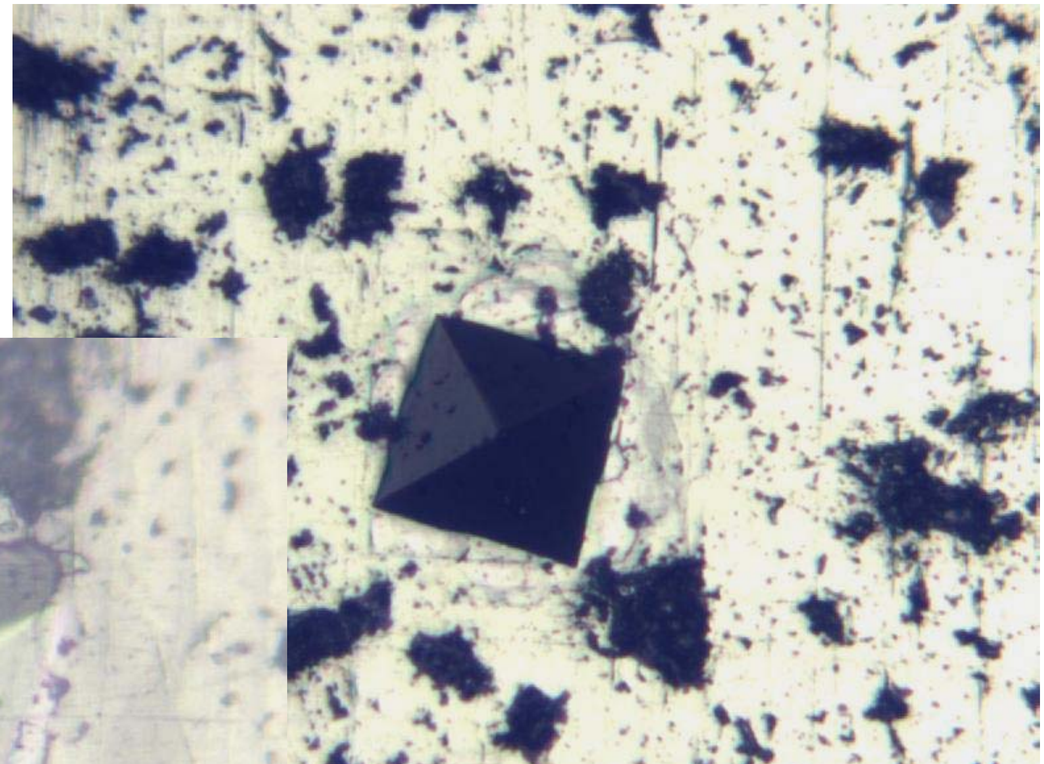

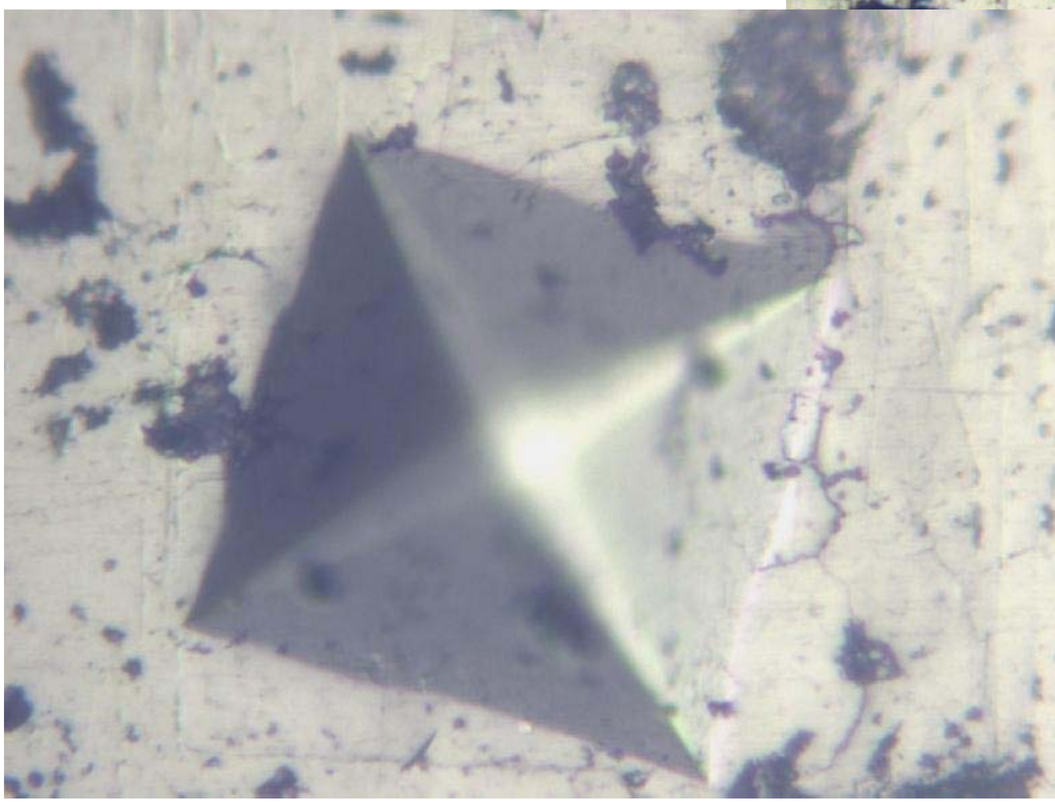

#678, Mo-3.4wt%$MgAl_2O_4$, Vickers Hardness

215HV, 1Kg, 30S

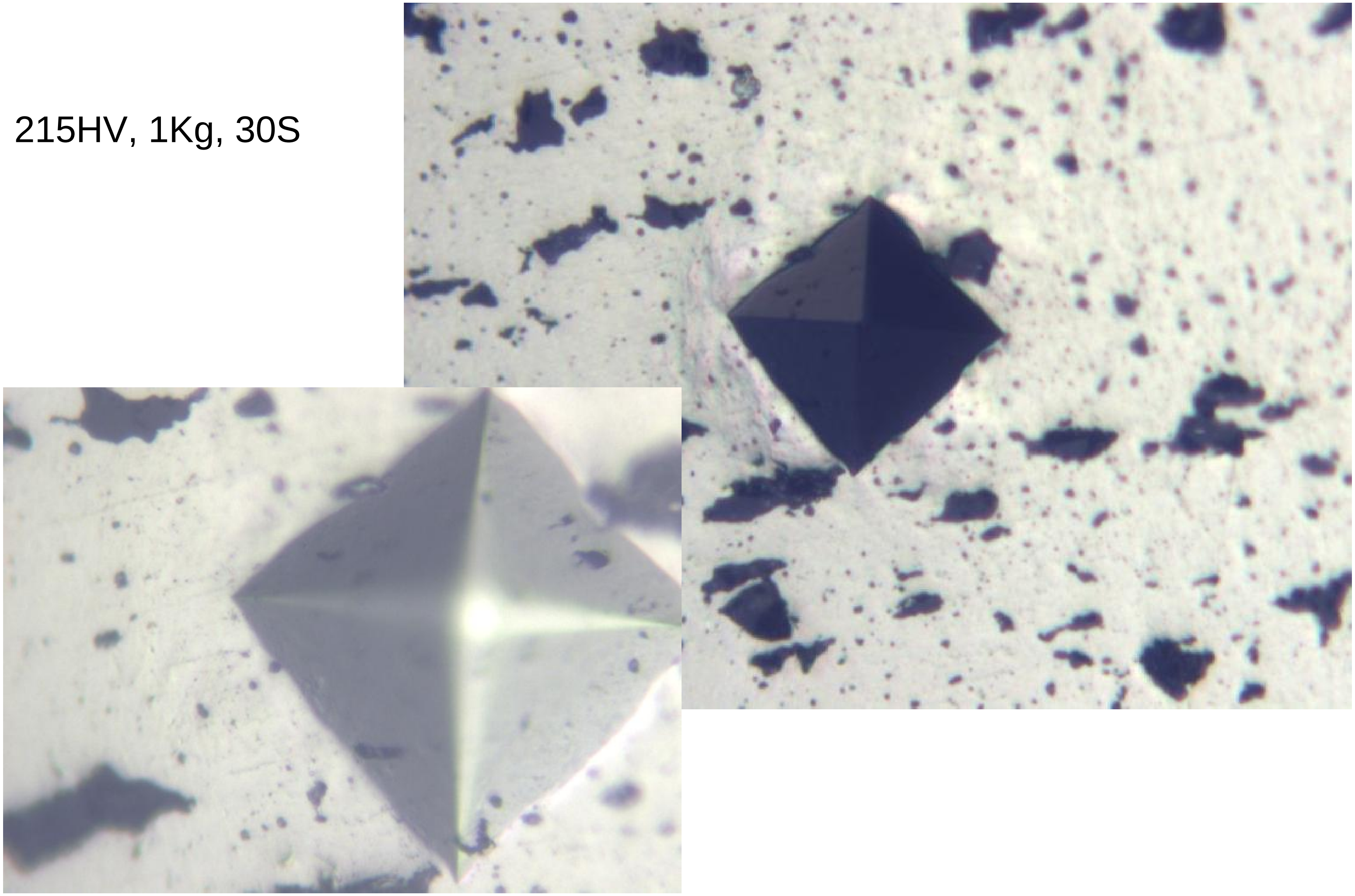

#696, Mo-3.0wt%$MgAl_2O_4$, Vickers Hardness

214HV, 1kg, 30s

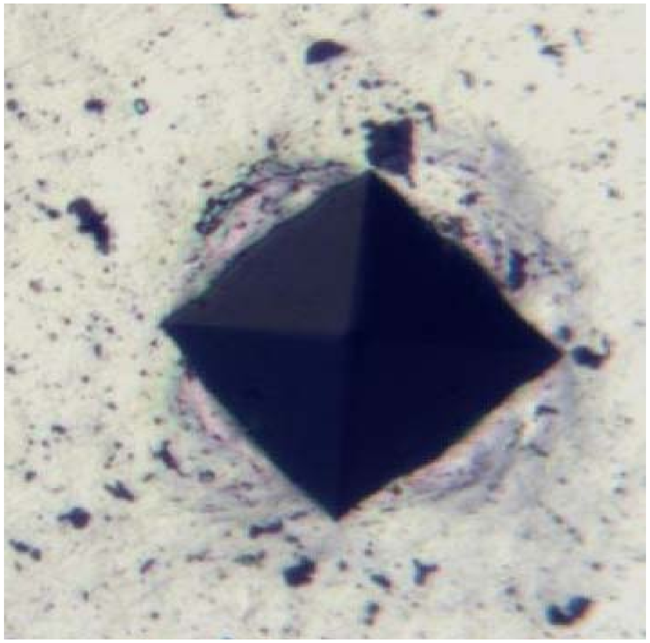

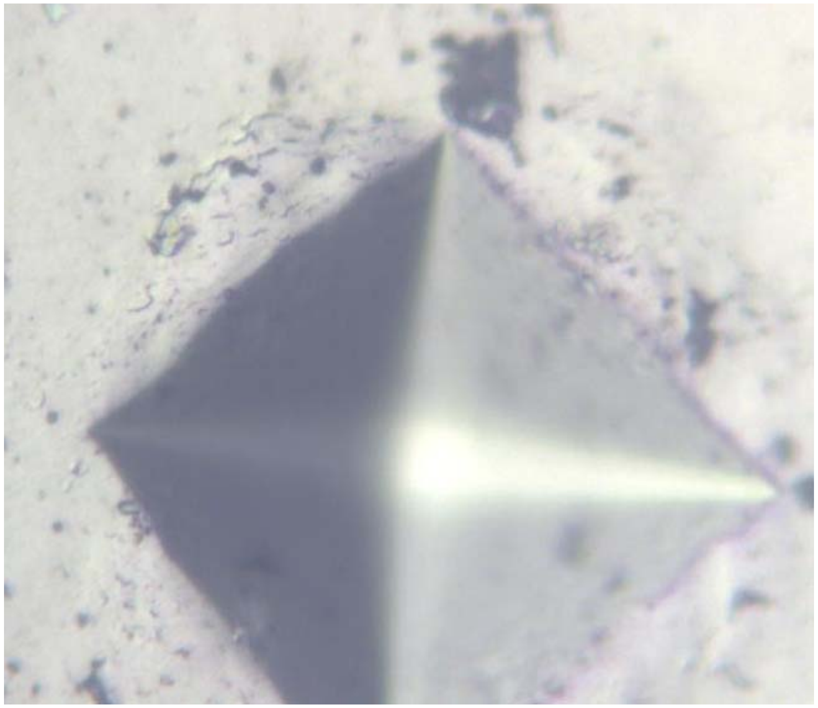

#698, Mo-3wt%MgO, Vickers Hardness

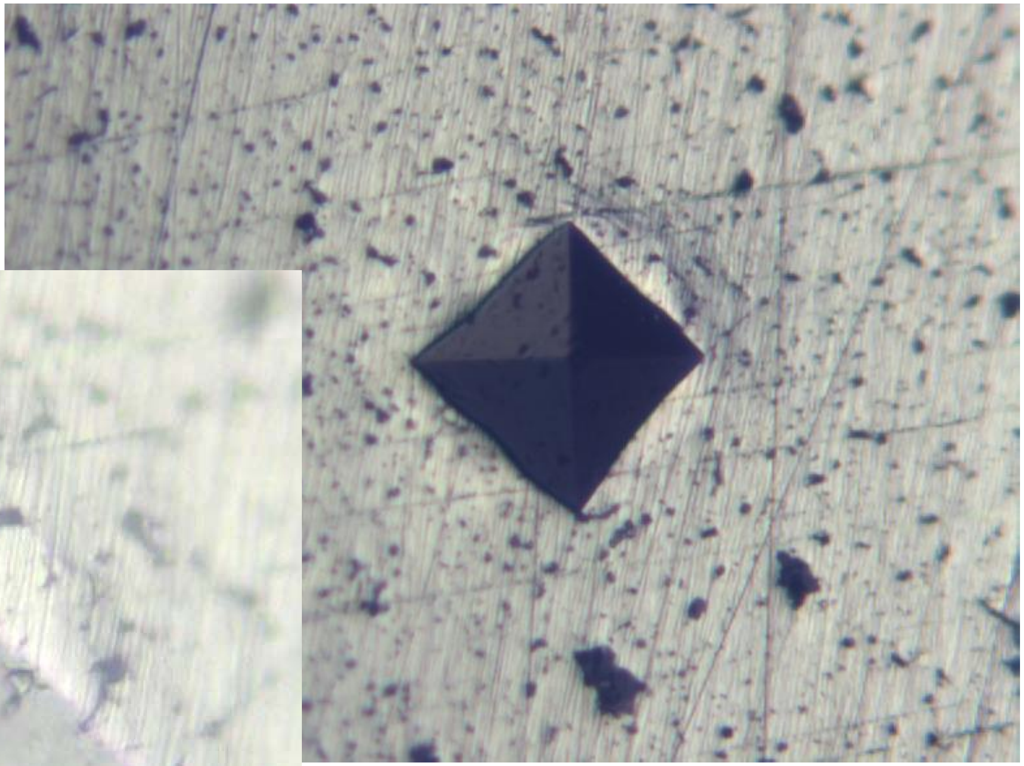

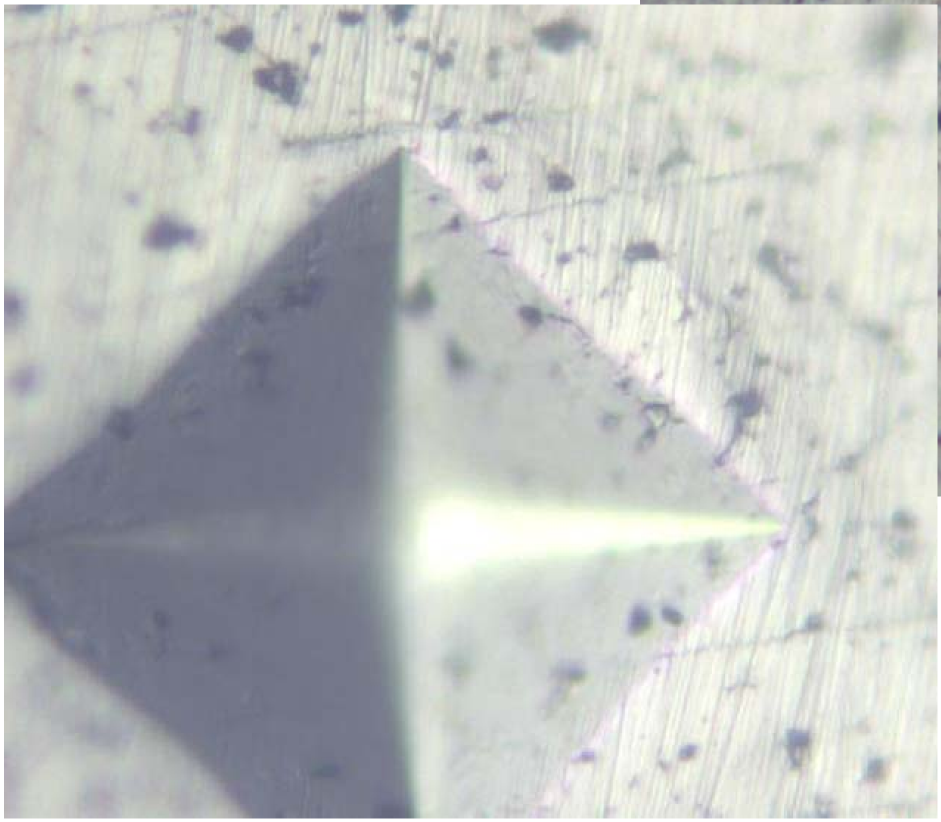

Indentation Fatigue
Mo alloy #697

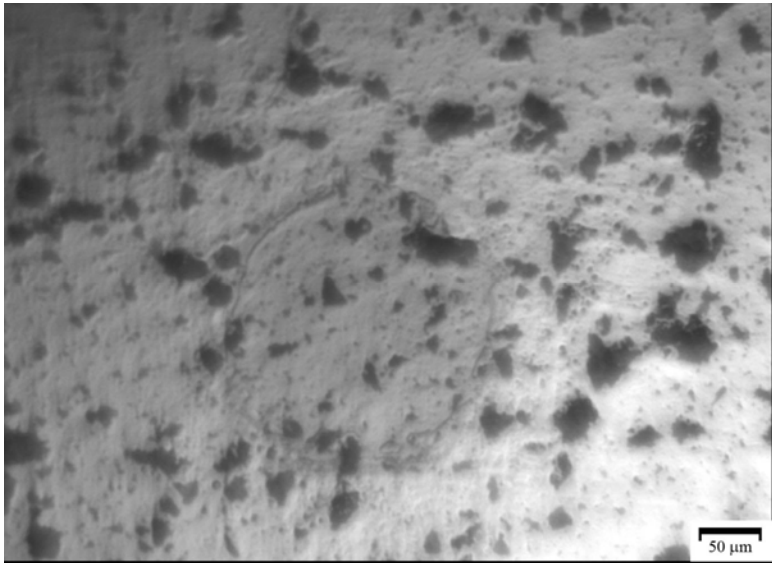

Loading.

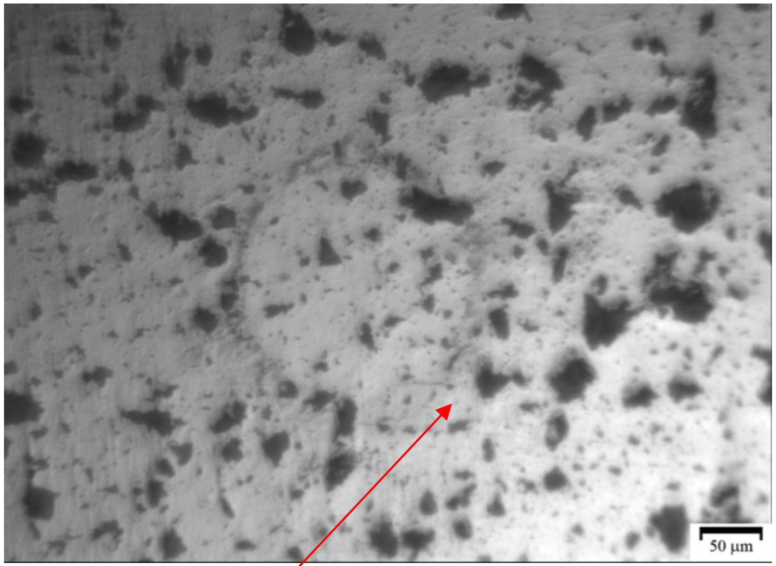

Unloading.

- $S_{nominal}/S_{yield}$ = 0.95
- S_{yield} = 300MPa, $S_{nominal}$ = 285MPa, 10 Hz.
- Failure occurred after ~600,000 cycles.

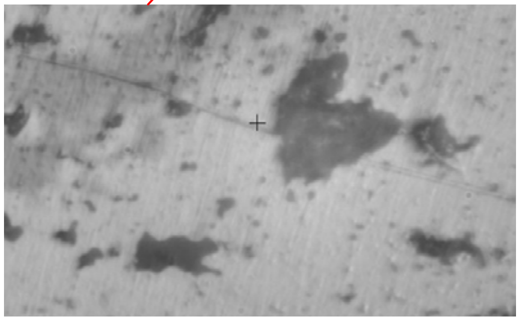

after ~600,000 cycles.